2020

Preliminary Study of Highway Pavement and Materials

Omer Eljairi
Claremont Graduate University

Preliminary Study of Highway Pavement and Materials

by

Omer Eljairi

Joint Doctoral Program in Engineering & Industrial Applied Mathematics

Claremont Graduate University/California State University-Long Beach

2020

APPROVAL OF THE REVIEW COMMITTEE

This dissertation has been duly read, reviewed, and critiqued by the Committee listed below, which hereby approves the manuscript of Omer Eljairi as fulfilling the scope and quality requirements for meriting the degree of Doctor of Engineering & Industrial Applied Mathematics.

Dr. Shadi Saadeh, Chair
California State University-Long Beach
Professor of Civil Engineering and Construction Engineering Management

Dr. Marina Chugunova, Committee Member
Claremont Graduate University
Professor of Mathematics, Program Director

Dr.Vahid Balali, Committee Member
California State University-Long Beach
Assistance Professor of Civil Engineering and Construction Engineering Management

Dr. Ali Nadim, Committee Member
Claremont Graduate University
Professor of Mathematics

ABSTRACT

Preliminary Study on Highway Pavement and Materials

by
Omer Eljairi

Joint Doctoral Program in Engineering & Industrial Applied Mathematics

Claremont Graduate University/California State University-Long Beach: 2020

This preliminary study covered (a) the effects of in-place air voids and other factors on fatigue cracking using Long-Term Pavement Performance data, (b) fracture properties of asphalt concrete in a semicircular bend (SCB) test using a noncontact camera and crosshead movement, and (c) hot applied modified-binder-chip-seal field performance in California. The objective is to improve pavement performance and life, establish a quality assurance/quality control (QA/QC) tests of fracture properties of asphalt mixtures, and save millions of dollars on maintenance and rehabilitation.

Chapter 1 investigated the effect of in-place air voids (AV), asphalt content (AC), bulk-specific gravity (BSG), and maximum specific gravity of asphalt (Gmm) on fatigue cracking. Including 72 sections from different locations covering mix designs, pavement age between 20 and 30 years, and two U.S. climate zones, the investigation included a multiple linear regression, and the random forest (RF) method between the selected explanatory factors and fatigue cracking. Regression models confirmed significant relationships between AC, AV, Gmm, percent of aggregate Pass.No.200, BSG, and fatigue cracking. Fatigue cracking aligned with high

AV, low BSG, low Gmm, and a low percentage of aggregate Pass.No.200. RF indicated that AC, Gmm, percent of aggregate Pass.No.200, and BSG are important factors.

Chapter 2 showed the SCB test is quick, indicative, and has reasonable variability in calculating crack propagation indirectly using crosshead movement (CHM) or crack mouth opening. A noncontact camera (NCC) and CHM were used to compared SCB. A strong correlation emerged between J_c from SCB NCC and J_c from SCB CHM, and between K_{1c} from SCB NCC and K_{1c} from SCB CHM. The SCB CHM test showed great potential as a quality assurance/quality control (QA/QC) test of fracture properties.

Chapter 3 assessed current conditions of the 14 Caltrans modified-binder seal-coat projects that contained some crumb rubber modification, and to determine their field performance. Field reviews between September and October 2015 found most projects were rated either good or fair. Primary distress types were transverse cracking, bleeding, and longitudinal cracking. Streaking and roping due to improper application rate/construction were observed. Transverse cracking and bleeding were the dominant distresses in high-mountain and high-desert regions.

Table of Contents

Table of Figures

Table of Tables

CHAPTER 1

EFFECTS OF IN-PLACE AIR VOIDS AND OTHER FACTORS ON FATIGUE CRACKING USING LTTP DATA

The primary objective of this study was to investigate the effect of in-place air voids (AV), asphalt content (AC), bulk specific gravity (BSG), and maximum specific gravity of asphalt (Gmm) on the fatigue cracking using Long-Term Pavement Performance (LTPP) program data. Although studies have shown the primary cause of fatigue cracking is excessive traffic loading, they have tended to focus less on other factors including mix design and aggregate properties that may affect the rate of this pavement distress. This study included 72 sections from different locations covering different mix designs, pavement age between 20 and 30 years, and two climate zones across the United States. All data derived from the LTPP database. A multiple linear regression, and the random forest (RF) method between selected explanatory factors and fatigue cracking were used for the investigation. Three multiple significant linear regressions models (A, B, and C) were developed and confirmed the significant relationships between AC, AV, Gmm, percent of aggregate Pass.No.200, BSG and fatigue cracking. The RF method was established using the same data, which validated significant factors and the accuracy of the models A, B, and C. RF indicated that AC, Gmm, percent of aggregate Pass.No.200, and BSG are important factors. However, because a correlation emerged between AV and the BSG, RF result showed that AV has a negative value of increase in mean squared error (%IncMSE).

The LTPP program was established to help understand how and why pavements perform as they do (Elkins, Thompson, Ostrom, Simpson, & Visintine, 2017). Such knowledge will help extend pavement life and save millions of dollars. The LTPP program aims to obtain knowledge

of the specific effects of various design features, traffic, environment, materials, construction quality, and maintenance practices on pavement performance. The LTPP collects and stores data from more than 2,500 test sections throughout the United States and Canada and is one of the largest pavement-performance experiments. The LTPP database is annually updated and publicly accessible (Elkins et al., 2017).

One of the most widespread and detrimental distresses found in asphalt pavements is fatigue cracking. Also known as alligator or long-term cracking, fatigue cracking has numerous negative effects on the short-term and long-term performance of asphalt pavements (Brown et al., 2009). If left untreated, this distress can ultimately lead to complete structural failure of an asphalt pavement. Typically, fatigue cracking occurs later in the life of asphalt pavement and is primarily caused by excessive traffic loading or loads above pavement design strength (Brown et al., 2009). However, other factors, including mix design, may affect the rate of this pavement distress (Haider & Chatti, 2009; Khattak & Peddapati, 2013; Zelelew, Senn, & Papagiannakis, 2012).

Zelelew et al. (2012) focused on identifying the causes of pavement failures of selected Arizona specific-pavement-5 test sections. One main distress identified in their study was fatigue cracking. High-severity fatigue cracking was observed in some test sections, perhaps due to high AVs in AC layers. The authors also found that rutting aligned with high binder content and AVs.

Haider and Chatti (2009) presented the results of a study on the relative influence of design features and site factors on the fatigue performance of in-service flexible pavements. Their findings supported the existing understanding of pavement-fatigue performance, suggesting that base type was the most significant factor affecting fatigue cracking. Haider and Chatti also indicated that base thickness has a negligible effect on fatigue-cracking performance

and cold weather has a significant effect. Their study provided an overview of the interactions between design and site factors and presented new insights on various design options to achieve better long-term pavement performance.

Khattak and Peddapati's (2013) research focused on the performance of flexible pavements and their relationship to in-situ mechanistic and volumetric properties. They studied 116 flexible pavement sections throughout the United States using the LTPP database. Their findings indicated that fatigue life is a function of tensile strain at the bottom of the hot-mix asphalt (HMA) layer, peak surface deflection, HMA AVs and maximum specific gravity, and ambient air temperature.

Ker, Lee, and Wu (2008) found the prediction accuracy of existing fatigue-cracking models was inadequate and greatly in need of improvement. The authors presented fatigue-cracking models using the LTPP database. Their model included factors such as pavement age, annual precipitation, annual temperature, critical tensile strain under the AC, surface layer, and freeze–thaw cycle for the predication of the fatigue-cracking layer. The proposed model appears to include substantial improvements over previous models.

Park and Kim (2015) conducted a field study in North Carolina to investigate the primary causes of fatigue cracking. Their study suggested that specific mix-design properties may impact fatigue cracking. The pavement tends to be in better condition with higher asphalt content and low AVs. Also, fine-graded mixes tend to yield a better pavement condition than coarse-graded mixes.

Two points emerged from this brief literature review. First, most reported effects of AV content and other factors on pavement performance have been based on laboratory evaluations or short-term field performance. Therefore, it would be useful to increase understanding of fatigue-

cracking effects on asphalt pavements using and studying the available data in the LTPP, which will help in developing more accurate models for pavement performance.

Second, little quantitative and systemic analysis exists of interaction effects of in-place AVs and AC, BSG, and Gmm on fatigue cracking. In addition, limited direct studies or experiments emerged for any correlations between any particular mix-design property and fatigue cracking. Based on findings from the literature review, studying the relationship between the mix design and aggregate properties with fatigue cracking appeared to be plausible, worthwhile, and significant.

Objective

The primary objective of this study was to investigate the effect of in-place AVs, AC, BSG, Gmm, the percent of aggregate passing through the No. 4 sieve, and the percent of aggregate passing through the No. 200 sieve on fatigue cracking of asphalt mixtures using the LTPP. Because most models of fatigue cracking prediction were based on laboratory results, it is important to use the LTPP to better understand pavement behavior. This study results determined if these properties affected the rate of fatigue cracking and how this knowledge can be used to create a statistically significant model that predicts fatigue cracking behavior in asphalt pavements.

Methodology

The data used in this analysis accrued from the LTPP InfoPave database. To limit the influence of outside factors on the data, I applied several filters: (a) only asphalt pavements between the ages of 20 and 30 years were included because it is widely known that pavement age is a primary influence in fatigue cracking; (b) the analysis was limited to include only pavements

in dry, nonfreeze, and wet zones with an annual temperature range between 0 and 30 degrees Celsius; and (c) roadways that have undergone rehabilitation were excluded from this analysis.

In this study, several key measured properties of aggregates used in asphalt mixtures included BSG and the absorption of coarse (CA) and fine aggregates (FA), the uncompacted void content of FA, the percent of aggregate passing through the No. 4 sieve, and the percent of aggregate passing through the No. 200 sieve. The method of measurement for each design property used in the study was as follows: The percent of AVs in asphalt concrete was calculated from cored asphalt concrete pavement samples (Simpson, Schmalzer, & Rada, 2007); to minimize possible variation of AV content due to wheelpath compaction, this study considered only AV measurements taken in the vehicle wheelpath.

For AC, I used the average AC. The BSG and maximum specific gravity of asphalt concrete derived from LTPP tests on asphalt cores. Also, data for the BSG and absorption value (Ab) of CA and FA, uncompacted void content of FA, the percent of aggregate passing through the No. 4 sieve, and the percent of aggregate passing through the No. 200 sieve accrued from the extracted aggregate test results. These test results were gathered at the initial construction.

In the LTPP InfoPave database, asphalt concrete pavement distresses are sorted into two major categories: Manual Distress and Highway Performance Monitoring System (HPMS)/Mechanistic-Empirical Pavement Design Guide (MEPDG) Distress. For this study, I chose the HPMS/MEPDG Distress category because these guidelines define fatigue cracking as a percentage. In this distress-assessment category, two sources define the asphalt-fatigue-cracking percentage. The first cracking percentage is defined by the 2016 edition of the HPMS Field Manual (Elkins et al., 2017). The second method of measurement is defined by the American

Association of State Highway and Transportation Officials in the MEPDG. In this study, I used only MEPDG cracking.

Finally, every pavement structure studied in the LTPP is given a unique identification number in the InfoPave database. This numbering system was originally developed by the Strategic Highway Research Program (SHRP); thus, the unique identification number for each pavement structure is known as an SHRP ID (Miller & Bellinger, 2003). For all tables produced in this study, each roadway is identified by its state and SHRP ID.

The methodology used in this study is summarized as follows:

- Collect data for all properties from the LTPP database.
- Run a multiple linear regression analysis using Minitab software between asphalt-pavement properties and fatigue cracking. From this analysis, develop statistically significant linear models to predict fatigue cracking.
- Use the RF regression method to validate and show significant factors on fatigue cracking. This method validates the accuracy of the multiple regression models developed to predict fatigue cracking. The RF method was established using commercial software R (The R Foundation, 2019).

Data Collection

As mentioned previously, all data used in this study were obtained from the LTPP InfoPave database. The first major step in this analysis was to reduce and sort the pavement data. I paired the selected properties according to their respective SHRP ID and state.

It was necessary to average several properties because the SHRP gave more than one data point for each pavement structure. After creating tables for each of the mix-design properties, the data needed to be combined into one concise table. If data were unavailable for either the

cracking or mix properties for any pavement structure, I excluded the pavement. Table 1 shows all previously discussed properties for each specific pavement structure with ages between 20 and 30 years. Data were only available for 13 pavements for all selected asphalt and aggregate properties.

To create a larger sample size, one or more of the mix or aggregate properties needed to be eliminated. The categories with the fewest number of data points were the uncompacted void content of FA and BSG and the absorption of CA and FA. The elimination of the restricting factors expanded the sample size to 72 distinct pavements, shown in Table 2.

Table 1

Percent Cracking vs. All Mix Design and Aggregate Properties

State	SHRP ID	% AV	AC (%)	Gmm	BSG	BSG of CA	Abs of CA	BSG of FA	Abs of FA	% Pass. No. 4	% Pass. No. 200	Uncomp. void	MEPDG %
Mississippi	806	6.77	5.31	2.40	2.25	2.55	0.82	2.62	0.62	55.73	4.88	41.81	10.90
New Mexico	801	8.58	7.00	2.21	2.00	2.22	4.10	2.44	1.97	58.67	6.60	48.63	6.07
Oklahoma	114	4.57	4.20	2.48	2.37	2.23	0.40	2.67	0.40	56.00	3.50	41.10	8.21
Oklahoma	115	4.63	4.60	2.44	2.37	2.63	0.50	2.66	0.70	44.00	7.60	44.13	2.50
Oklahoma	116	5.16	5.00	2.46	2.34	2.63	0.52	2.64	0.52	49.00	5.72	41.86	6.07
Oklahoma	117	6.64	3.70	2.52	2.33	2.67	0.30	2.67	0.40	41.00	5.30	41.57	3.00
Oklahoma	121	10.2	3.59	2.50	2.30	2.62	0.50	2.67	0.50	63.00	4.10	41.37	7.57
Oklahoma	123	7.99	2.80	2.52	2.32	2.63	0.43	2.67	0.30	29.75	3.48	40.78	4.79
Texas	801	5.98	4.95	2.44	2.29	2.48	0.80	2.50	1.45	62.00	4.10	42.22	0.21
Texas	802	5.43	4.82	2.43	2.30	2.49	0.65	2.51	1.30	61.25	4.02	42.63	0.64
Virginia	117	5.53	5.03	2.42	2.21	2.57	0.60	2.60	0.65	53.50	5.80	45.63	9.44
Virginia	118	4.72	4.30	2.37	2.26	2.63	0.40	2.60	0.50	41.00	4.50	45.02	10.60
Virginia	119	8.81	4.33	2.45	2.21	2.61	0.44	2.61	0.50	42.39	5.38	45.45	4.33

Note. SHRP = Strategic Highway Research Program, AV = air void, AC = asphalt content, Gmm = maximum specific gravity of asphalt, BSG = bulk-specific gravity, CA = coarse aggregates, Ab = absorption value, %Pass No.4 = the percent of aggregate passing through the No. 4 sieve, %Pass No.200 = the percent of aggregate passing through the No. 200 sieve, Uncomp = uncompacted void content, MEPDG% = fatigue cracking percentage using Mechanistic-Empirical Pavement Design Guide.

Table 2

Percent Cracking vs. Reduced Mix Design and Aggregate Properties.

State	SHRP ID	% AV	AC (%)	Gmm	BSG	% Pass. No. 4	% Pass. No. 200	MEPDG %
Alabama	3998	6.78	4.90	2.51	2.34	62.30	2.35	0.20
Alabama	6019	7.42	4.57	2.47	2.29	57.00	4.87	0.00
Arizona	260	8.83	4.30	2.54	2.36	54.00	4.40	4.92
Arizona	261	5.75	4.70	2.52	2.39	59.00	5.60	11.9
Arizona	1002	4.72	5.96	2.54	2.43	56.30	5.71	0.00
Arizona	1007	3.50	4.82	2.48	2.39	47.60	4.75	7.88
Arizona	6053	2.20	4.60	2.34	2.29	68.80	6.75	0.00
California	2040	9.02	4.30	2.49	2.26	55.50	5.10	5.60
California	2051	8.15	4.90	2.51	2.30	48.50	5.85	10.4
Florida	3995	6.53	5.60	2.37	2.21	61.00	4.75	8.00
Florida	3996	1.80	6.10	2.33	2.29	62.00	5.10	21.00
Florida	4106	6.09	6.25	2.32	2.18	59.50	3.75	3.43
Florida	9054	3.99	6.15	2.33	2.24	65.50	3.55	1.50
Georgia	1031	4.38	5.02	2.49	2.39	53.50	7.05	0.08
Georgia	4096	8.15	4.77	2.52	2.30	60.30	7.73	2.25
Georgia	4112	3.83	5.16	2.43	2.33	44.00	3.38	0.00
Georgia	4113	4.10	4.73	2.45	2.35	42.80	3.80	1.00
Georgia	7028	2.10	4.92	2.47	2.42	52.80	7.00	0.20
Hawaii	1003	6.77	5.58	2.59	2.40	64.80	12.67	0.75
Hawaii	1006	7.73	5.65	2.54	2.34	60.80	12.67	4.25
Hawaii	7080	7.38	5.75	2.63	2.43	61.00	8.40	0.43
Mississippi	806	6.77	5.31	2.40	2.25	55.70	4.88	10.90
New Jersey	1034	3.84	5.02	2.51	2.40	54.50	5.50	13.60
New Jersey	1638	6.34	4.54	2.51	2.35	53.80	4.97	12.80
New Mexico	801	8.58	7.00	2.21	2.00	58.70	6.60	6.07
New Mexico	1005	2.40	5.30	2.41	2.36	61.00	6.05	0.00
New Mexico	1112	6.38	5.05	2.58	2.41	63.50	7.75	0.00
New Mexico	6401	5.18	5.37	2.47	2.34	57.80	8.50	13.50
Oklahoma	114	4.57	4.20	2.48	2.37	56.00	3.50	8.21
Oklahoma	115	4.63	4.60	2.44	2.37	44.00	7.60	2.50
Oklahoma	116	5.16	5.00	2.46	2.34	49.00	5.72	6.07

State	SHRP ID	% AV	AC (%)	Gmm	BSG	% Pass. No. 4	% Pass. No. 200	MEPDG %
Oklahoma	117	6.64	3.70	2.52	2.33	41.00	5.30	3.00
Oklahoma	121	10.22	3.59	2.50	2.30	63.00	4.10	7.57
Oklahoma	123	7.99	2.80	2.52	2.32	29.80	3.48	4.79
Oklahoma	1015	3.34	3.35	2.51	2.44	40.50	6.25	5.43
Oklahoma	4088	6.78	4.43	2.47	2.34	61.00	8.37	8.00
Oklahoma	4163	5.08	4.26	2.51	2.39	52.00	6.31	2.67
Oklahoma	4165	5.64	4.21	2.50	2.36	62.00	6.44	1.69
Oklahoma	6010	6.43	5.09	2.42	2.26	58.10	8.47	3.40
Tennessee	3101	7.62	4.57	2.52	2.35	55.80	8.68	1.50
Tennessee	6015	5.54	4.07	2.54	2.38	45.30	7.20	0.50
Tennessee	6022	6.14	3.48	2.52	2.39	32.30	4.55	0.00
Tennessee	9025	6.51	4.86	2.52	2.35	60.00	9.00	2.75
Texas	801	5.98	4.95	2.44	2.29	62.00	4.10	6.07
Texas	802	5.43	4.82	2.43	2.30	61.30	4.02	0.64
Texas	1039	5.53	4.40	2.47	2.32	51.50	3.75	15.3
Texas	1047	3.45	3.85	2.47	2.38	39.00	5.70	1.57
Texas	1048	3.81	5.55	2.35	2.28	43.00	12.00	2.75
Texas	1065	4.75	4.40	2.45	2.34	50.50	6.05	5.75
Texas	1069	2.20	4.40	2.44	2.38	58.30	4.73	9.11
Texas	1070	4.20	4.60	2.42	2.32	50.50	4.30	3.43
Texas	1174	12.12	6.25	2.21	1.94	54.50	7.45	8.86
Texas	1181	11.08	8.05	2.14	1.90	46.00	8.70	16.30
Texas	1183	5.69	5.45	2.33	2.20	41.50	6.90	0.60
Texas	2133	6.09	4.90	2.42	2.27	59.50	6.25	4.63
Texas	3559	5.62	3.85	2.49	2.35	67.00	7.90	0.00
Texas	3729	2.33	5.42	2.39	2.33	50.00	7.17	8.00
Texas	3739	4.88	5.80	2.38	2.26	62.00	6.00	0.56
Texas	6079	5.88	5.07	2.45	2.31	59.80	5.83	11.30
Texas	6086	7.10	4.10	2.43	2.21	55.00	9.50	0.00
Texas	9005	5.67	4.55	2.46	2.33	50.50	4.45	7.07
Virginia	115	6.88	4.86	2.41	2.22	36.00	4.36	2.50
Virginia	117	5.53	5.03	2.42	2.21	53.50	5.80	3.00
Virginia	118	4.72	4.30	2.37	2.26	41.00	4.50	10.60
Virginia	119	8.81	4.33	2.45	2.21	42.40	5.38	4.33
Virginia	124	9.73	4.07	2.44	2.26	41.80	3.41	5.56

State	SHRP ID	% AV	AC (%)	Gmm	BSG	% Pass. No. 4	% Pass. No. 200	MEPDG %
Virginia	159	7.99	5.20	2.44	2.22	52.00	5.60	8.00
Washington	801	5.00	6.05	2.51	2.37	59.00	7.25	6.07
Washington	802	10.69	5.50	2.53	2.32	48.00	6.20	0.64
Washington	1002	1.89	4.65	2.46	2.42	54.00	7.30	0.00
Washington	1801	3.23	5.48	2.43	2.35	60.50	6.27	1.67
Washington	6049	6.10	5.77	2.47	2.32	59.80	5.90	4.00

Note. SHRP = Strategic Highway Research Program, AV = air void, AC = asphalt content, Gmm = maximum specific gravity of asphalt, BSG = bulk-specific gravity, %Pass No.4= the percent of aggregate passing through the No. 4 sieve, %Pass No.200= the percent of aggregate passing through the No. 200 sieve, MEPDG % = fatigue cracking percentage using Mechanistic-Empirical Pavement Design Guide.

Data Analysis

Multiple Regression Result

I used a multiple regression analysis using Minitab to determine if a statistically significant regression model could be developed to correlate mix design and aggregate properties to percent fatigue cracking in asphalt pavements using LTPP data. For all models, the research (or alternative) hypothesis was that a significant model could exist between these properties and percent of fatigue cracking. The null hypothesis, therefore, declared that a significant model did not exist between these quantities. To test the hypothesis, a level of significance of .05 was used.

I made many attempts to develop a model that incorporated all the mix design and aggregate properties. The data shown in Table 1 were used to develop the multiple regression model for the 13 pavement structures. The maximum specific gravity of asphalt (Gmm), the Abs of CA and the percent passing sieve No. 4 had *p*-values greater than the designated level of significance (.05). Therefore, I removed these properties and reconstructed the model. This iteration of the multiple regression analysis yielded Model A, which was statistically significant for the overall model and each of the predictors shown in Table 3 and Equation 1. Figure 1 verifies the assumption that the residuals are normally distributed because the points follow a

straight line. Therefore, the multiple regression model closely fits the presented data. The adjusted R^2 is equal to 97.82%.

Table 3

Coefficients for Model A

Term	Coef.	SE coef.	95% CI	*t*-value	*p*-value
Constant	-617.230	67.760	(-805.370, -429.090)	-9.110	0.0008
% AV	-1.158	0.195	(-1.699, -0.617)	-5.940	0.0040
AC (%)	6.813	0.598	(5.151, 8.475)	11. 380	0.0003
BSG	-33.425	7.018	(-52,911 -13.939)	-4.760	0.0089
BSG of CA	24.971	2.851	(17.057, 33.886)	8.760	0.0009
BSG of FA	209.690	19.240	(156.260, 263.120)	10.900	0.0004
Abs of FA	16.035	2.477	(9.158, 22.912)	6.470	0.0029
% Passing No. 200	-6.735	0.573	(-8. 328 -5.142)	-11.740	0.0003
Uncompacted void	2.019	0.286	(1.225, 2.814)	7.060	0.0021

Note. AV = air void, AC = asphalt content, BSG = bulk-specific gravity, CA = course aggregates, FA = fine aggregates, %Pass No.4 = the percent of aggregate passing through the No. 4 sieve, %Pass No.200= the percent of aggregate passing through the No. 200 sieve.

$$MEPDG\% = -617.230 - 1.158\%AV + 6.813AC\% - 33.425BSG + 24.971BSG\ of\ CA + 209.690BSG\ of\ FA + 16.035Abs\ \ of\ FA - 6.735\%\ \text{Passing No. 200} + 2.019Uncomp.Void \quad (1)$$

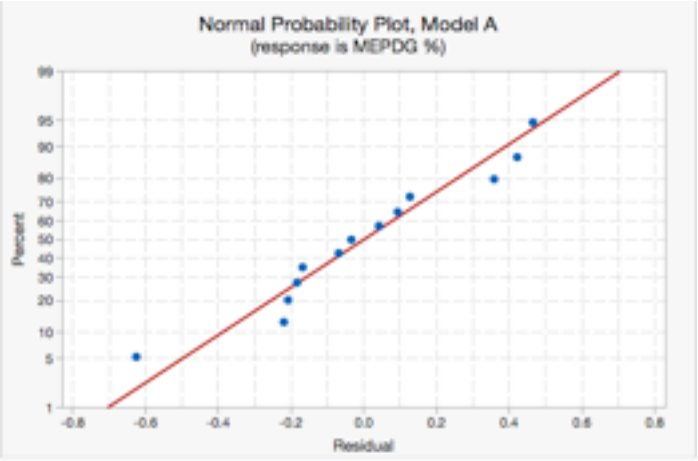

Figure 1. Normal probability plots: Model A.

Second, I attempted to develop a model that incorporated the data shown in Table 2. These data represented a significantly larger number of pavement structures, so I expected it to produce a model with a higher level of reliability. For the first step of this modeling process, I used the best subsets tool in Minitab to determine which properties (i.e., predictors) would best represent cracking (i.e., response). From the best-subsets output, two potentially significant models emerged. The first, Model B, incorporated the percent AV, the Gmm, and the BSG. The second model, Model C, only used the asphalt content and the percent finer than the No. 200 sieve. The *p*-value was .0017 for the overall variance of Model B. In addition, the *p*-value was less than .05 for each of the predictors, as shown in Table 4 and Equation 2. This result signified that Model B is statistically significant for the given data. Also, the adjusted R^2 value for this model is 24.44%. Figure 2 indicates that the multiple regression model closely fit the presented data.

Table 4

Coefficients for Model B

Term	Coef.	*SE* Coef.	95% CI	*t*-value	*p*-value
Constant	20.350	11.680	(-3.210,43.910)	1.740	0.088
% AV	1.887	0.604	(0.668, 3.106)	3.120	0.003
Gmm	-54.260	20.620	(-95.850, -12.670)	-2.680	0.012
BSG	45.180	21.100	(2.630, 87.740)	-2.140	0.038

Note. AV = air void, Gmm = maximum specific gravity of asphalt, BSG = bulk specific gravity.

$$MEPDG\% = 20.350 + 1.887\%AV - 54.260Gmm + 45.180BSG \quad (2)$$

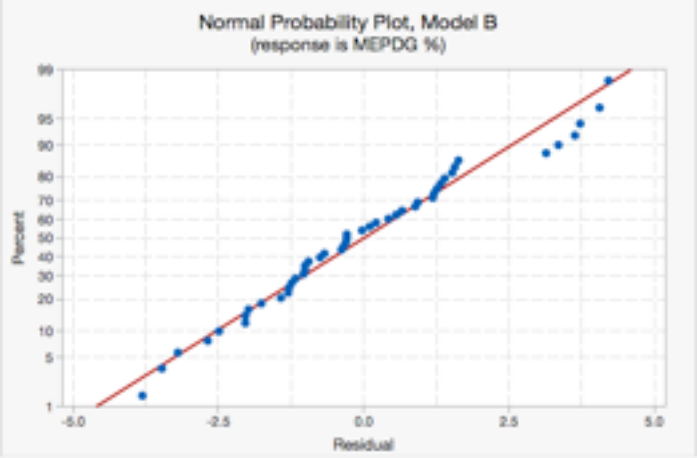

Figure. 2. Normal probability plots: Model B.

Model C was also developed using Table 2 data that attempted to correlate AC and the percent of aggregate passing through the No. 200 sieve in a similar manner. Model C yielded a *p*-value less than .05 for the overall model variance and for each predictor, as shown in Table 5 and Equation 3. This model had an adjusted R^2 value of 20.81%. Model C had the lowest adjusted R^2 value compared to Models A and B. However, it had the largest amount of data and fewer outliers than Model B. This result indicates that the model somewhat resembles the percent of cracking. Figure 3 also indicates that the multiple regression model closely fits the presented data because the residuals are normally distributed and follow the straight line.

Table 5

Coefficients for Model C

Term	Coef.	SE coef.	95% CI	*t*-value	*p*-value
Constant	11.406	2.587	(6.190,16.623)	4.410	0.0001
AC (%)	-1.223	0.479	(-2.189, -0.256)	-2.550	0.0143
% Passing No. 200	-0.522	0.186	(-0.897, -0.147)	-2.810	0.0074

Note. AC = asphalt content.

$$MEPDG\% = 11.406 - 1.223\%AC - 0.5223\%Pass.No.200 \quad (3)$$

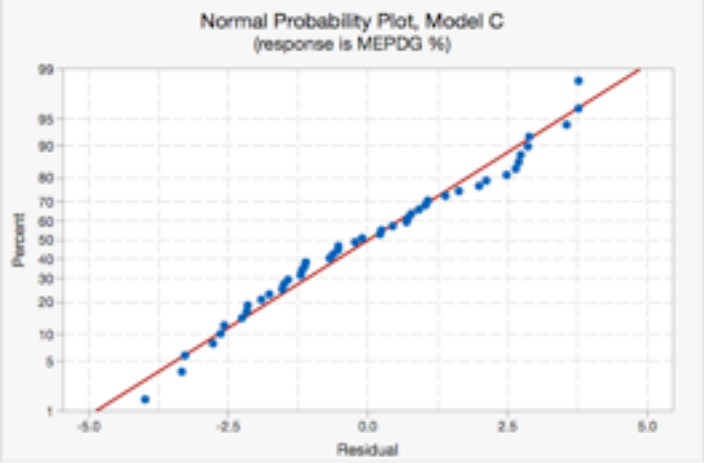

Figure. 3. Normal probability plots (Model C).

Random Forest Result

RF regression was used to validate the multiple linear regression method and to show the significant factors on the fatigue cracking of asphalt mixtures. It was also used to investigate if a multicollinearity problem arose between explanatory properties. RF is a machine-learning method to classify and regress, introduced by Breiman and Cutler (1984). Many researchers discussed the concept of RF regression (Breiman & Cutler, 1984.; Svetnik et al., 2003). This method builds on an ensemble of decision trees from which the prediction of a continuous variable is provided as the average of the predictions of all trees. In this study, the number of tress in the forest (ntree) is 500 and the number of different descriptors tried at each split (mtry) is 1 (Géron, 2017). I performed this method using commercial software R (The R Foundation, 2019).

I ran the RF method using data from Tables 1 and 2. Figures 4 and 5 show RF important properties plotted from Tables 1 and 2, respectively. From Figure 4, Abs of FA, BSG of CA BSG of FA, BSG, and AC properties show a positive increase in %IncMSE, which confirms

significant relationships between these properties and fatigue cracking. It appears that AV, uncompacted void and the percent of aggregate passing through the No. 200 sieve have negative %IncMSE. This result could be due to a multicollinearity problem between AV and another explanatory property. I obtained a correlation matrix to determine the reason for such a result. The correlation matrix showed a high correlation between AV and BSG and between uncompacted void and BSG. This explains why AV, uncompacted void, and the percent of aggregate passing through the No. 200 sieve have negative %IncMSE. Therefore, in addition to having a significant *p*-value and high R^2 for Model A, this confirms the significance of Model A, which can be used for fatigue-cracking prediction.

Shown in Figure 5, the RF method confirmed that AC, BSG, Gmm, and the percent of aggregate passing through the No. 200 sieve are significant properties for fatigue cracking because they have positive values of %IncMSE. This result validated the accuracy of Model C because it has the important properties of AC and the percent of aggregate passing through the No. 200 sieve. However, AV and the aggregate passing through the No. 4 sieve have negative %IncMSE values. I used a correlation matrix to evaluate this result, as it is inconsistent with Model B. The correlation matrix showed that a correlation between AV and BSG justified obtaining the negative value of %IncMSE for AV. Therefore, RF results also validated the accuracy of Model B to predict fatigue cracking.

Conclusion

This study examined the effects of in-place AV, AC, BSG, and Gmm, the percent of aggregate passing through the No. 4 sieve, and the percent of aggregate passing through the No. 200 sieve on the field fatigue cracking of asphalt mixtures. A multiple linear regression between the properties and fatigue cracking was conducted to predict fatigue cracking using the data

shown in Tables 1 and 2. In addition, the RF method was established using R software to validate and show the significant properties that affect fatigue cracking. Based on the analysis results, the following conclusions can be drawn:

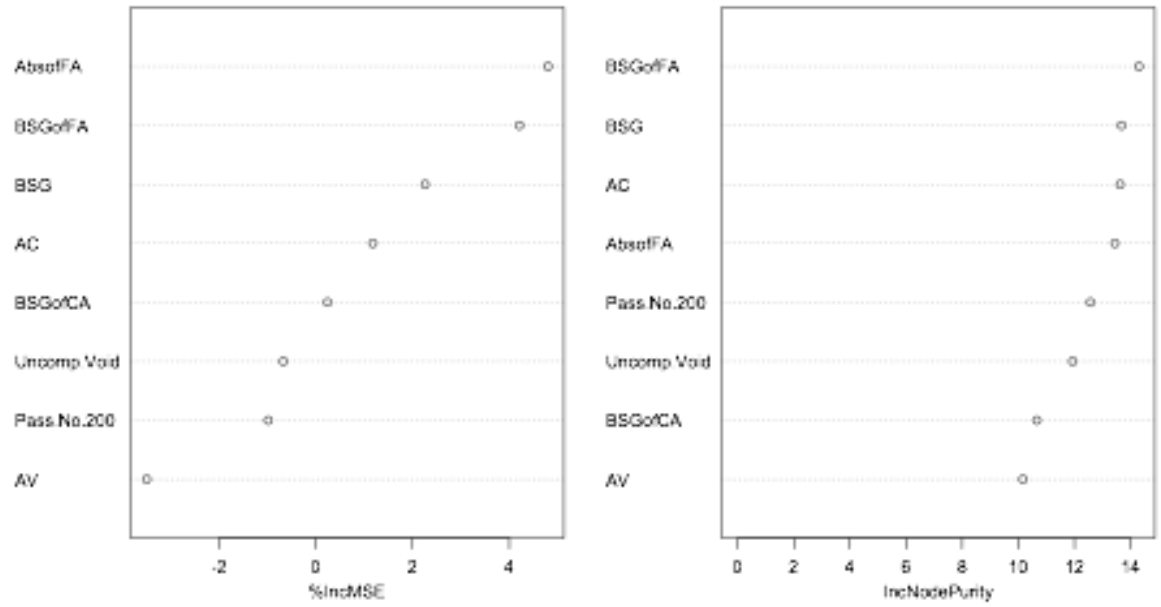

Figure. 4. Variable important measure of the random forest from data in Table 1.

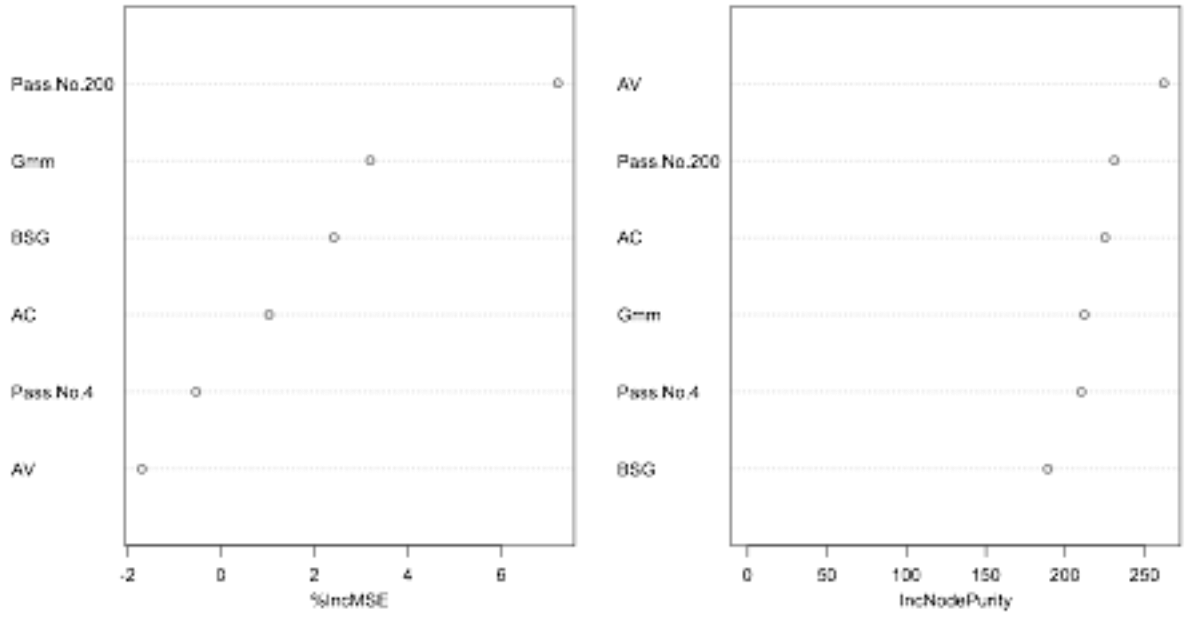

Figure. 5. Variable important measure of the random forest from data in Table 2.

- Three significant models (A, B, and C), developed from the multiple linear regressions, predicted fatigue cracking.
- Model A has the largest number of variables, the strongest fit, and the highest coefficient of determination, indicating AV, AC, BSG, BSG of CA, BSG of FA, Abs of FA, the percent of aggregate passing through the No. 200 sieve, and uncompacted void significantly impacted fatigue cracking.
- Model B indicated that AV, BSG, and Gmm significantly impacted fatigue cracking.
- Model C showed that AC and aggregate passing through the No. 200 sieve significantly impacted fatigue cracking.
- RF confirmed that AC, Gmm, percent of aggregate passing through the No. 200 sieve, and BSG are important properties, and AV and the aggregate passing through the No. 4 sieve have a negative value in %IncMSE. This result could be due to a correlation between AV with BSG. Therefore, this result validated the accuracy of Models A, B, and C and they can be used to predict fatigue cracking.
- Not only traffic loading is the cause of fatigue cracking, but also mix design and aggregate properties affected the rate of the cracking because the three linear regressions models (A, B, and C) confirmed significant relationships between the AC, AV, Gmm, percent of aggregate passing through the No. 200 sieve, BSG, and fatigue cracking.
- I recommend this analysis be revisited after more data has been added to the LTPP InfoPave database because the number of available samples was limited for the data used to develop Model A.

- I recommend investigating how the results of this analysis would change for pavements outside the age range used in this study.

CHAPTER 2

Comparison of Fracture Properties of Asphalt Concrete in the Semicircular Bend Test Using Noncontact Camera and Crosshead Movement

The semicircular bend (SCB) test has received a great deal of attention in recent years. The test is quick, indicative, and has reasonable variability compared to other fracture-property tests for asphalt concrete (AC) mixtures. The crack propagation in the test is calculated indirectly using the crosshead movement (CHM) or crack mouth opening (CMO). Although these methods might correlate well to crack propagation, little research has ascertained this relationship. The main objective of this chapter is to compare the SCB test using a noncontact camera (NCC) and CHM. a comprehensive comparison of fracture properties of six AC mixtures, captured by these two methods was conducted. I determined the critical strain energy release rate (J_c) and the critical fracture toughness (K_{1c}) values for AC mixtures. A strong correlation emerged between J_c from SCB NCC and J_c from SCB CHM, and between K_{1c} from SCB NCC and K_{1c} from SCB CHM. The Study results indicated that the SCB CHM test has great potential as a quality assurance/quality control (QA/QC) test of fracture properties of asphalt mixtures.

Fatigue resistance of AC is defined as the ability of the AC to resist repeated traffic loading without significant cracking or failure (Harvey, Deacon, Tsai, & Monismith, 1995). Fatigue cracking is a primary distress in asphalt concrete due to repetitive stress and strain caused by traffic loading. a number of fatigue tests were developed to investigate the fatigue resistance of AC. Fatigue cracking is often associated with loads that are too heavy for a pavement structure. Fatigue cracking is also associated with many repetitions of a given load (Roberts, Kandhal, Brown, Lee, & Kennedy, 2009).

Zhou, Hu, and Scullion (2007) presented the Texas overlay test (OT), which researchers at the Texas Transportation Institute developed to assess fatigue-cracking predictions. Wagnoner, Buttlar, and Paolino (2005) developed the disk-shaped compact tension test as a practical method to obtain the fracture energy of asphalt concrete.

Chong and Kuruppu (1984) proposed to use a semicircular core specimen with a single-edge notch, subjected to three-point loading. In recent years, the SCB test has become more popular as a way to determine the fracture properties of AC. Hofman, Oostcrbaan, Erkens, and Kooji (2003) found that the cyclic SCB test was very promising in determining the constants for the Paris law of crack propagation (Paris & Erdogan, 1963).

Wu, Mohammad, Wang, and Mull (2005) used the SCB test to analyze the fracture resistance of 13 superpave mixtures. They used an elastoplastic-fracture-mechanics concept of critical-strain-energy release rate, also called the critical value of J-integral (J_c). They concluded that the J_c value depended on the binder and the nominal maximum size.

Mohammad, Kabir and Saadeh (2008) and Kim, Mohammad, and Elseifi (2012) investigated the use of SCB and indirect-tension tests to correlate fracture properties with cracking properties of asphalt mixtures. Results showed a good correlation between the SCB J_c value, the indirect tension toughness index, and field-cracking performance data. In addition, the asphalt-binder grade and aging condition of specimens influenced the fracture properties of asphalt mixtures.

Saadeh, Eljairi, Kramer, and Hajj (2012) investigated the influence of moisture on the fracture properties of asphalt mixtures. They conducted 24 SCB tests on wet and dry California asphalt mixtures, performing the tests at 20°C. The results were quite reliable; however, they recommended more tests on different AC mixtures to obtain more definitive results.

Hakimelahi, Saadeh, and Harvey (2013) investigated the fracture properties of seven AC mixtures using the beam-fatigue test (BFT) and SCB test. Hakimelahi et al. indicated a good correlation between SCB J_c with BFT number of load cycles to failure (N_f), and plateau-value (PV) parameters. The researchers showed a poor correlation exists between BFT initial stiffness and SCB J_c, BFT N_f, and PV. Mahmoud, Saadeh, and Hakimelahi (2013) used SCB test results to develop and calibrate an extended finite element model, (XFEM) coupled with cohesive zone modeling (CZM). They developed XFEM-CZM the model was then used to investigate crack propagation in SCB and to predict SCB simulations for experimental results not used in the calibration process. The model calibration had very good alignment with the experimental results and the model successfully predicted SCB testing results.

SCB test has been used in many pavement-material studies to investigate the fracture properties of AC mixtures (Arabani & Ferdowsi, 2009; Mohammad et al., 2003; Mohammad, Wu, & Aglan, 2004; Molenaar, Scarpas, Liu, & Erkens, 2002; Mull, Stuart, & Yehia, 2002; Othman, 2011; Saha & Biligiri, 2017; Zeng, Yang, Chen, & Bai, 2016). Clearly, SCB is receiving significant attention as a candidate to investigate the fracture properties of AC. The crack propagation in the test is calculated indirectly using the CHM or crack mouth opening (CMO). Although these methods might correlate well to the crack propagation, little research has been done to ascertain this relationship.

Objective

The main objective of this study was to compare the SCB test using an NCC and CHM to validate the CHM method, thereby allowing researchers to investigate the use of the SCB test as a QA/QC measure for field construction and to investigate the feasibility of using SCB test results as a trigger for further investigation. This objective was achieved by testing six asphalt

mixtures: mixtures with recycled-asphalt pavement (RAP), warm-mix asphalt (WMA), lime, and PM asphalt.

Scope

Six AC mixtures types (performance gradePG64-10RAP [LIME], PG64-28modifiedPM [LIME], 710P4-AR, AN-HMA, AN-WMA, and WMA-ADVERA) were tested in this study using SCB. The crack length propagation was estimated using two methods, CHM and NCC. the same specifications and methodology were used to prepare cores for SCB testing. To determine the value of J_c, semi-circular specimens with at least two different notch depths need to be tested for one mixture. three notch depths 25.4, 31.8, and 38.0 mm (1, 1.25, and 1.5 in.) were used in this study.

Methodology

In this study, I conducted the SCB test using an NCC and CHM to validate the CHM method. To achieve this goal, I selected six AC mixtures used in California. I selected various asphalt mixtures with various gradation and mixture designs to achieve a comprehensive comparison and evaluation.

Material Properties and Mixture Design

I conducted a total of 36 SCB CHM method tests on six asphalt mixtures (PG64-10RAP [LIME], PG64-28PM [LIME], 710P4-AR, AN-HMA, AN-WMA, WMA-ADVERA). In addition, I conducted 18 SCB NCC tests on the same six mixtures.

Table 6 provides information about the mixture properties used in this study. As presented in Table 6, I used two methods of mix design: SHRP Level 1 and Caltrans' Type A_19 mm (California Department of Transportation, 2015b; SHRP, 2017). I fabricated samples using

two methods: laboratory-mixed laboratory-compacted and field-mixed field-compacted. As can be seen in Table 6, aggregates were provided from different sources.

Table 6

Hot-Mix Asphalt Mixtures Properties.

Mix type	Binder type	Mix design	Aggregate source	Specimen preparation type
PG64-10RAP (lime treated)	PG64-10 (Valero)	SHRP Level 1 mix design	Red Bluff (District 2)	LMLC
PG64-28PM (lime treated)	PG64-28PM (Valero)	SHRP Level 1 mix design	Red Bluff (District 2)	LMLC
710P4-AR	AR-8000 (PG64-16)	Caltrans' Hveem	San Gabriel River Valley at Azusa	LMLC
AN-HMA	PG64-10 (Valero-Benicia)	Caltrans' Hveem	Graniterock-Wilson Quarry	LMLC
AN-WMA	PG64-10 (Valero-Benicia)	Caltrans' Hveem	Graniterock-Wilson Quarry	LMLC
WMA-ADVERA	PG64-16 (Valero-Benicia) with Advera warm mix	Caltrans' Hveem	Graniterock-Wilson Quarry	FMFC

Note. PG = performance grade, PM = polymer-modified, RAP = recycled-asphalt pavement, AR = asphalt rubber, HMA = hot-mix asphalt, WMA = warm-mix asphalt, SHRP = Strategic Highway Research Program, LMLC = lab-mixed lab-compacted, FMFC = field-mixed field-compacted.

SCB Test

The SCB test is used to characterize the fracture resistance of asphalt mixtures based on a fracture-mechanics concept. SCB test specimens were loaded monotonically until achieving fracture under a constant cross-head deformation rate of 5 mm/min (0.02 in/min). I used a three-point bend-load configuration, as shown in Figure 6. The test duration was typically under 10 minutes. More details on the procedure can be found in the National Cooperative Highway Research Program (2016) and Mohammad et al. (2008). In this study, I measured SCB test parameters based on two methods: CHM and NCC. I determined the J_c for each mixture tested

using CHM and NCC methods. I also used another parameter, K_{1c}, determined according to Hofman et al. (2003). The scheme of a typical test specimen appears in Figure 7. the tests at 20°C (as in Harvey et al., 1995).

Figure 6. Semicircular-bend test set-up.

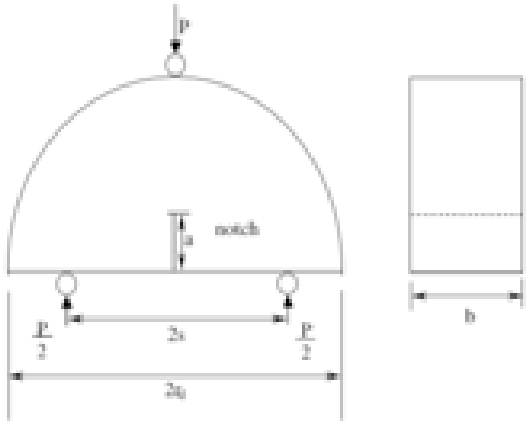

Figure 7. Semicircular-bend test specimen scheme.

SCB Test CHM Method

I used six different AC mixtures in this study and designed a specific name for each mixture replicate. Table 7 presents test factorials for the SCB test. I used two replicates, represented by the letters “A” and “B.”

The maximum load (F_{max}), at which the specimen failed, was determined. The load and deformation were continuously recorded and the critical value of J-integral and K_{1c} were determined using the following equations:

$$J_c = -\left(\frac{1}{b}\right)\frac{\partial U}{\partial a} \quad [1]$$

Where "*b*" is sample thickness, "*a*" is initial notch depth, and "*U*" is the strain energy generated up unril failure i.e. the area up to fracture under the load-deflection plot.

$$\sigma_{max} = \frac{4.263.F_{max}}{D.t} \quad [2]$$

$$K_{1c} = \sigma_{max}\sqrt{\pi a} f\left(\frac{a}{W}\right) \quad [3]$$

Where

$$f\left(\frac{a}{W}\right) = -0.623 + 29.29\left(\frac{a}{W}\right) - 171.2\left(\frac{a}{W}\right)^2 + 457.1\left(\frac{a}{W}\right)^3 - 561.2\left(\frac{a}{W}\right)^4 + 265.54\left(\frac{a}{W}\right)^5$$

and "σ_{max}" is the maximum stress, "F_{max}" is the maximum load, "K_{1c}" is the fracture toughness, "*a*" is the initial notch depth and "*W*" is the specimen height. Hofman et al., (2003) determined the correlation factor "*f*" through 2D finite element analysis.

Table 7

Semicircular Bend Test Factorial

Mix type	Specimen designation		Notch size	AV (%)
PG64-10RAP (LIME)	3.15-HAM-RAP-64-10-5.38-1-1D	A	25.40	4.90
	3.15-HAM-RAP-64-10-5.38-1-1D	B	25.40	
	3.15-HAM-RAP-64-10-5.38-1-2C	A	31.75	5.50
	3.15-HAM-RAP-64-10-5.38-1-2C	B	31.75	
	3.15-HAM-RAP-64-10-5.38-2-1C	A	38.10	4.70
	3.15-HAM-RAP-64-10-5.38-2-1C	B	38.10	
PG64-28PM (LIME)	3.15-PG64-28PM-5.2-1-2C	A	25.40	5.20
	3.15-PG64-28PM-5.2-1-2C	B	25.40	
	3.15-PG64-28PM-5.2-1-3C	A	31.75	5.10
	3.15-PG64-28PM-5.2-1-3C	B	31.75	
	3.15-PG64-28PM-5.2-2-3C	A	38.10	4.90
	3.15-PG64-28PM-5.2-2-3C	B	38.10	
710P4-AR	710p4-AR-4.3-1-2C	A	25.40	6.10
	710p4-AR-4.3-1-2C	B	25.40	
	710p4-AR-4.3-1-3C	A	31.75	6.10
	710p4-AR-4.3-1-3C	B	31.75	
	710p4-AR-4.3-2-2C	A	38.10	6.30
	710p4-AR-4.3-2-2C	B	38.10	
AN-HMA	AN-WMA-DG-8-2B	A	25.40	4.60
	AN-WMA-DG-8-2B	B	25.40	
	AN-WMA-DG-8-3B	A	31.75	3.90
	AN-WMA-DG-8-3B	B	31.75	
	AN-WMA-DG-9-3A	A	38.10	6.30
	AN-WMA-DG-9-3A	B	38.10	
AN-WMA	AN-WMA-2-1B	A	25.40	6.00
	AN-WMA-2-1B	B	25.40	
	AN-WMA-6-1B	A	31.75	6.60
	AN-WMA-6-1B	B	31.75	
	AN-WMA-6-2B	A	38.10	6.90
	AN-WMA-6-2B	B	38.10	
WMA-ADVERA	WMA-A3-4T	A	25.40	9.10
	WMA-A3-4T	B	25.40	
	WMA-A18-4C	A	31.75	8.70
	WMA-A18-4C	B	31.75	
	WMA-A31-8C	A	38.10	8.40
	WMA-A31-8C	B	38.10	

Note. AV = air void, PG = performance grade, RAP = recycled-asphalt pavement, AR = asphalt rubber, HMA = hot-mix asphalt, WMA = warm-mix asphalt, PM = polymer-modified, DG = decomposed granite.

SCB Test NCC Method

During the SCB test, an NCC was fixed in front of the SCB specimen to measure crack length. This method, is called SCB NCC, measuring crack length using this method would be more accurate as it will account for the irregular crack length. Trilion Optical Test Systems provided the camera system (ARAMIS; see Figure 6). ARAMIS (1995) is an optical system used to measure complex materials and structures to determine their three-dimensional (3D) deformation and strain during loading. This tool is a full-field, noncontact strain-measuring testing device. The system offers a noncontact measurement of 3D deformation and strain using 3D image-correlation methods (digital image correlation, DIC) using high-resolution digital cameras with a charge-coupled device (CCD).

I used this method on the same specimens (simultaneously) that were analyzed using SCB CHM. The only difference between these methods was the way of measuring the crack length. The system records continuous frames of the test specimen as it undergoes monotonic loading. In addition, the camera can track full-field 3D-strain information. The system will interpolate between steps in time when crack growth is difficult to track or unknown at that stage. The Trilion Crack Processing software exports all images from ARAMIS. Before exporting, the visualization is set to either the major strain or the mises strain and the scale is fixed from 0 to 15% strain. Figure 8 shows an image frame, processed by software written in MATLAB (1984). The ARAMIS measurement field is limited to a 25.4 mm (1 in.) wide strip; in this study, it was set up such that the bottom of this strip was at the top of the specimen notch.

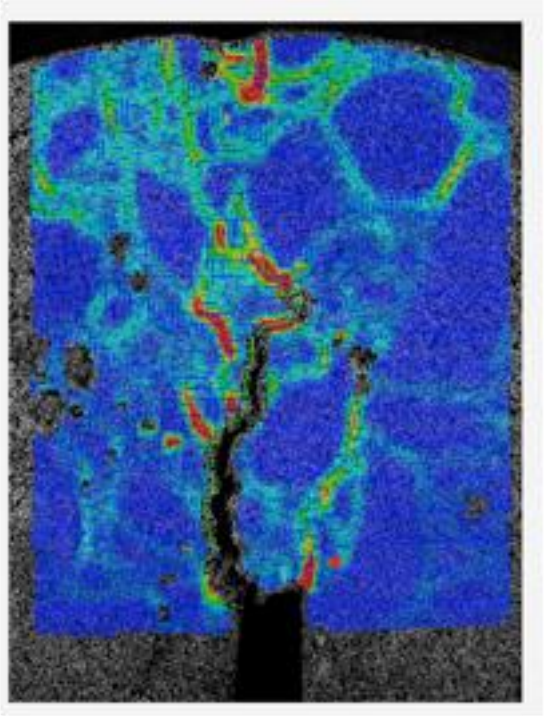

Figure 8. Crack processing software written in MatLAB.

Trilion has created a module that postprocesses the ARAMIS visualization to track crack growth over time. The cameras used in this study made it possible to measure irregular crack length at different stages of the test, as shown in Figure 9. seed points were placed at a stage of known crack growth (the last image before the test concluded). Because the crack was fully developed, the crack path was tracked as shown in Figure 10. After correlation between image number and the crack-tip position over time, the length of the crack is then measured using ARAMIS 3D coordinate information.

For each of the 18 specimens, the peak-strain values can be used to identify the location of the crack tip, as shown in Figure 11. the crack length at different stages was measured. a sixth-order polynomial correction was applied to the load signal to smooth the crack-length-versus-load chart, as shown in Figure 12. This technique was developed jointly with the Trilion Company.

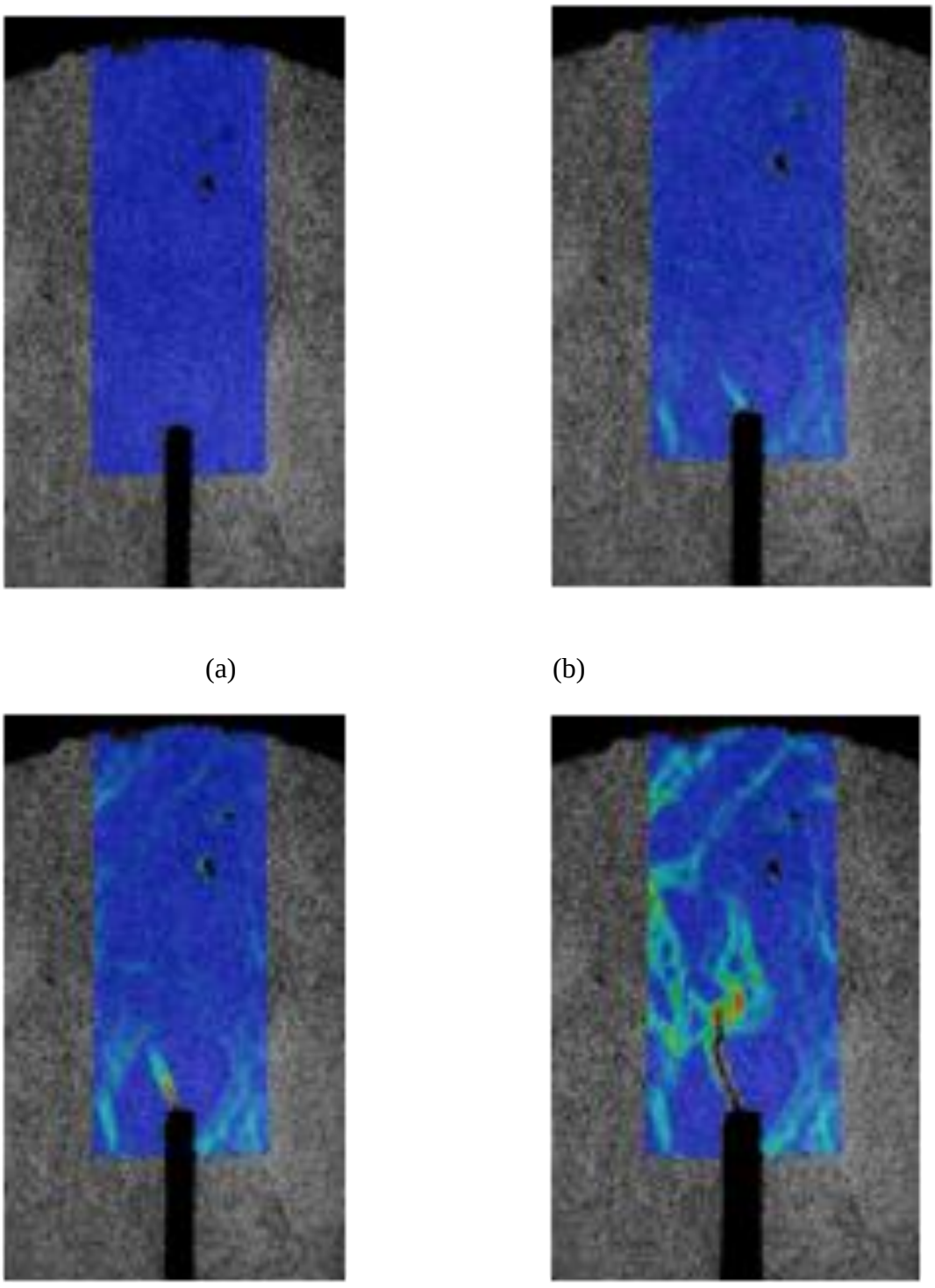

(a) (b)

(c) (d)

Figure 9. Semicircular-bend test-camera method procedure (a) Stage 1, (b) Stage 25, (c) Stage 38, (d) Stage 58, pictures were taken using (ARAMIS) camera system by Trilion Optical Test Systems Company.

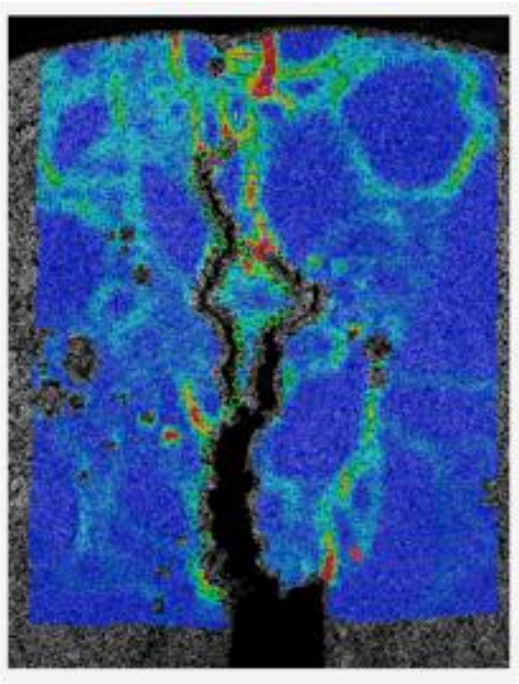

Figure 10. Tracking Backwards from known crack growth.

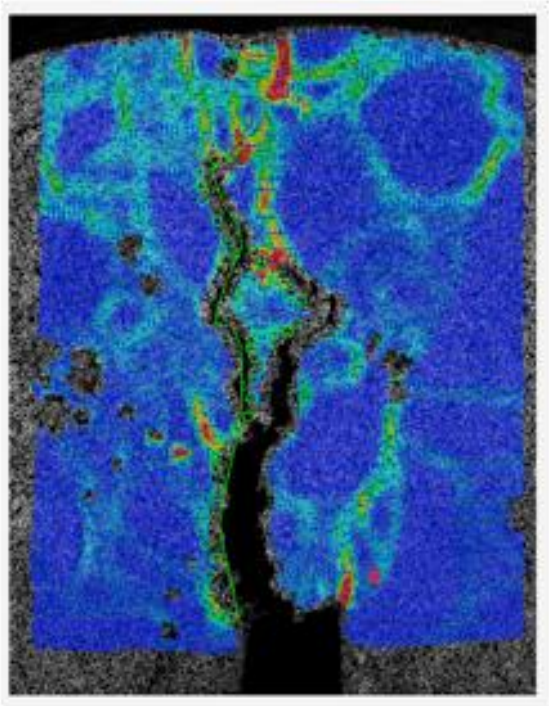

Figure 11. Identifying the crack tip.

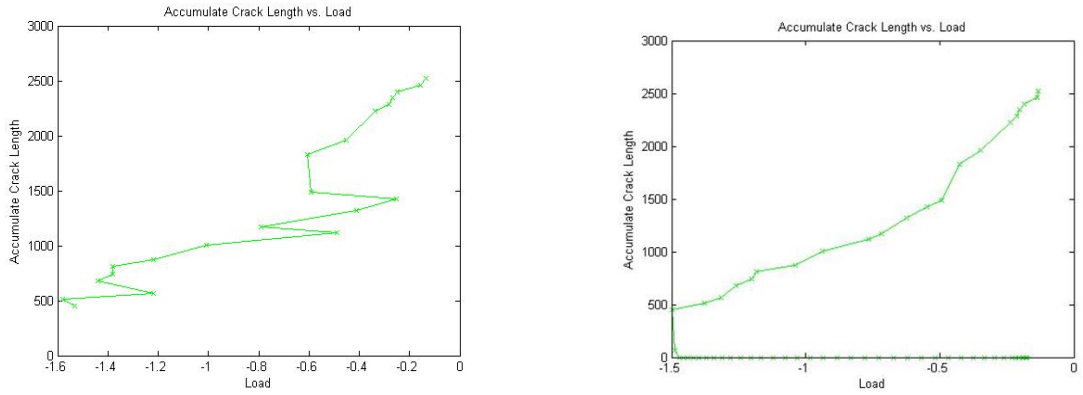

(a) (b)

Figure 12. 6th order correction is applied to the load signal for smoothing.

In the SCB NCC, the maximum load (F_{max}), *J*-integral, and K_{1c} were determined as described in the previous section. The results from the irregular crack measurement were compared to the SCB CHM. The comparison of these parameters provided better understanding of the SCB test and helped provide accurate measurement of the crack length.

Discussion of Results

SCB Test, CHM Method

A total of 36 SCB CHM tests were performed on six mixtures (PG64-10, PG64-28, 710P4-AR, AN-HMA, AN-WMA, and WMA-ADVERA) with three notch-depths 25.4, 31.8, and 38.0 mm (1, 1.25, and 1.5 in.), using two replicates each. In previous studies, researchers constructed load-displacement curves for three notch depths of AC mixtures for all mixtures (Mohammad et al., 2008). the maximum load (F_{max}) was recorded and the area under the load-displacement curve was used to determine the strain energy (*U*). the calculated strain energy for each notch was used to determine the critical strain energy J_c. By dividing the slope of the line of best fit to the specimen's thickness, the J_c value can be calculated. the calculated peak load and

the dissipated energy for each SCB test were used to determine the critical fracture toughness (K_{1c}) and J_c values (see Equations 1 and 3).

The SCB CHM J_c and K_{1c} values for each AC mixture appear in Table 8. The table presents the dissipated energy (U), the coefficient of variation (CV%), the critical value of J_c, and the ranking of the mixtures based on the J_c and K_{1c} parameters. The values of J_c ranged from 0.662 to 1.132 kN/m (7.9 to 13.60 lb/in). The values for K_{1c} ranged from 2.46 to 4.40 MPa/m$^{1/2}$. The presented values are the average of the calculated data and the coefficient of variation ranged from 0 to 38% for J_c and from 0 to 35% for K_{1c}.

Table 8

Semicircular Bend Crosshead Movement Test Results (J_c) and (K_{1c})

Mix type	Notch (mm)	U (kN.m)	CV%	J_c (kN/m)	Rank	K_{1c} (MPa/m$^{1/2}$)	Rank
PG64-10RAP	25.4	1.246	3	0.662	6	4.43	1
	31.75	1.032	1				
	38.1	0.797	10				
PG64-28PM	25.4	1.051	28	0.816	3	2.88	4
	31.75	0.749	18				
	38.1	0.498	26				
710P4-AR	25.4	1.543	11	1.132	1	4.12	2
	31.75	1.269	13				
	38.1	0.776	22				
AN-HMA	25.4	1.113	37	0.696	5	3.62	3
	31.75	0.81	15				
	38.1	0.642	21				
AN-WMA	25.4	1.155	17	0.866	2	2.46	6
	31.75	0.896	35				
	38.1	0.568	32				
WMA-ADVERA	25.4	1.069	4	0.711	4	2.69	5
	31.75	0.86	38				
	38.1	0.587	12				

Note. U = strain energy, CV% = coefficient of variation, J_c = critical strain release rate, K_{1c} critical fracture toughness, PG = performance grade, RAP = recycled-asphalt pavement, AR = asphalt rubber, HMA = hot-mix asphalt, WMA = warm-mix asphalt.

To better compare the ranking of J_c, I used an analysis of variance (ANOVA). Using ANOVA, the *p*-value determines whether the model is significant. Typically, researchers compare the *p*-value to an alpha value of .05. A *p*-value that is lower than alpha indicates that the model is significant. For J_c values, the *p*-value was .037 with 95% degree of confidence. I used the Tukey analysis, which is part of an ANOVA, to examine the difference in the groups with different rankings.

The Tukey analysis with 95% degree of confidence indicates that J_c values can be categorized in just one group. To compare test results, analysts need more than one group of test results. Therefore, the ANOVA for J_c values was performed at an 80% degree of confidence. As a result, J_c values were categorized in three separate groups. The compression of these three groups, with the mixtures' J_c ranking, indicates a direct correlation among J_c values, which ranked 1 and 2, 3 and 4, and 5 and 6 in Table 8 and these three groups.

Measured Accurately

Similar to J_c, I performed an ANOVA on K_{1c} values with a 95% degree of confidence. The *p*-value was 0, which indicated that K_{1c} was a significant parameter. Tukey analysis showed that the results for this parameter can be categorized into four different groups.

SCB Test, NCC Method

A total of 18 SCB tests with the NCC method were performed on six mixtures (PG64-10, PG64-28, 710P4-AR, AN-HMA, AN-WMA, and WMA-ADVERA) with three notch-depths (1, 1.25, and 1.5 inch).

The SCB NCC J_c and K_{1c} values for each AC mixture appear in Table 9. The value of J_c ranged from 0.226 to 1.559 kN/m. The value of K_{1c} ranged from 2.782 to 5.280 MPa /$m^{1/2}$.

Table 9

Semicircular Bend Noncontact Camera Test Results (J_c) and (K_{1c})

Mix type	Notch (mm)	*U* (kN.m)	J_c (kN/m)	Rank	K_{1c} (MPa/$m^{1/2}$)	Rank
PG64-10RAP	25.4	0.515	0.271	5	5.280	1
	31.75	0.273				
	38.1	0.331				
PG64-28PM	25.4	0.612	0.676	3	3.077	4
	31.75	0.187				
	38.1	0.153				
710P4-AR	25.4	0.995	1.137	2	4.848	2
	31.75	0.694				
	38.1	0.225				
AN-HMA	25.4	0.369	0.226	6	2.782	6
	31.75	0.255				
	38.1	0.216				
AN-WMA	25.4	1.226	1.559	1	2.971	5
	31.75	0.437				
	38.1	0.170				
WMA-ADVERA	25.4	0.311	0.281	4	3.255	3
	31.75	0.143				
	38.1	0.121				

Note. U = strain energy, J_c = critical strain release rate, K_{1c} critical fracture toughness, PG = performance grade, RAP = recycled-asphalt pavement, AR = asphalt rubber, HMA = hot-mix asphalt, WMA = warm-mix asphalt.

As with the SCB CHM method, I used an ANOVA to gain a better comparison of mixtures ranking. I used the Tukey analysis, which is part of an ANOVA, to examine the difference in the groups with different rankings. To categorize J_c and K_{1c} values, I performed a Tukey analysis with a 95% degree of confidence on the data. Test results ranking (J_c and K_{1c}), as well as ANOVA ranking for the mixtures, appear in Table 10.

Table 10

Semicircular Bend Noncontact Camera, Semicircular Bend Crosshead Movement Modified Rankings

Mix type	SCB NCC		SCB CHM	
	J_c	K_{1c}	J_c	K_{1c}
PG64-10RAP	4	1	4	1
PG64-28PM	3	4	2.67	3
710P4-AR	2	1	1	1
AN-HMA	4	4	4	2
AN-WMA	1	4	2.67	4
WMA-ADVERA	4	4	4	3

Note. SCB = semicircular bend, NCC = noncontact camera, CHM = crosshead movement, PG = performance grade, RAP = recycled-asphalt pavement, PM = polymer-modified, AR = asphalt rubber, WMA = warm-mix asphalt.

Comparison Between SCB CHM and SCB NCC

The SCB CHM and SCB NCC test results appear in Tables 8 and 9. I calculated J_c and K_{1c} values for both SCB test methods based on three-notch depths. Table 10 shows the ranking for the test parameters. I used the ANOVA and Tukey analysis to rank the AC mixtures. I converted the rankings to a scale from 1 to 4 to demonstrate the results in a figure. Incorporating the Tukey analysis provided better understanding of how the data were distributed.

I used the rankings to correlate the tests parameters to each other. Figure 13 presents the correlation between the SCB CHM and SCB NCC test rankings. In this figure, I plotted the J_c and K_{1c} values from the two SCB test methods. Figures 13a and 13b show a good correlation between the SCB NCC J_c and SCB CHM J_c with a correlation factor of 0.745 as well as SCB NCC K_{1c} and SCB CHM K_{1c} with a correlation factor of 0.852. The K_{1c} parameter was not able to clearly rank the mixtures to different categories in the Tukey analysis, which may have influenced the correlation of the parameter key.

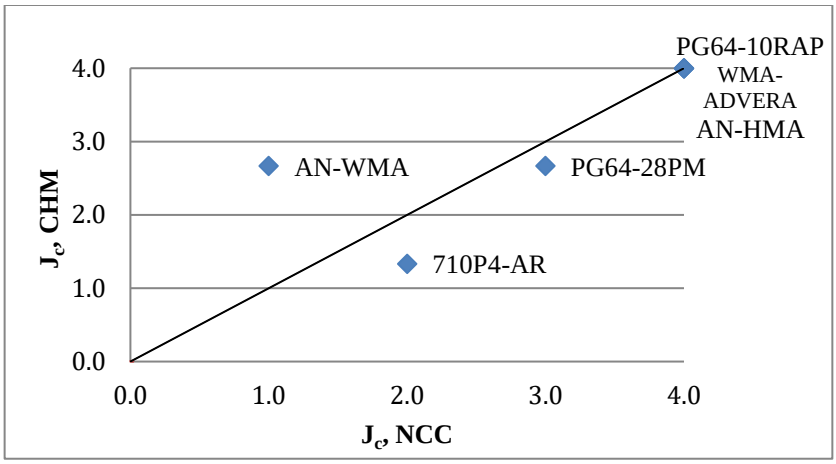

(a)

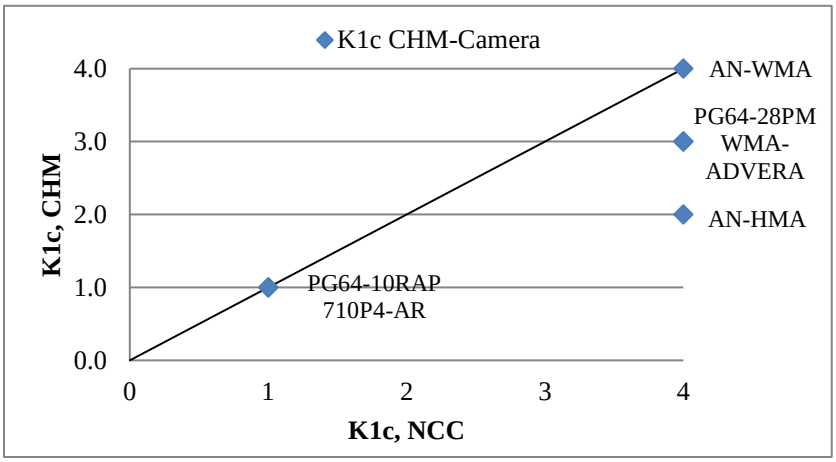

(b)

Figure 13. Semicircular bend crosshead movement and semicircular bend noncontact camera test results. Correlation (a) critical strain release rate crosshead movement, (b). critical fracture toughness crosshead movement–critical toughness crosshead movement noncontact camera.

Conclusions

I compared fracture properties of six AC mixtures under the SCB test using NCC and CHM. In the SCB test for both NCC and CHM methods, I determined the J_c and K_{1c} values for (PG64-10RAP [LIME], PG64-28PM [LIME], 710P4-AR, AN-HMA, AN-WMA, and WMA-ADVERA), mixtures.

The conclusions limited to this study follow:

- The CV% ranged from 0 to 38 for J_c and from 0 to 35 for K_{1c} in the SCB CHM.
- A strong correlation emerged between J_c from SCB NCC and SCB CHM J_c value and between K_{1c} from SCB NCC and SCB CHM K_{1c} value.
- The comparison between the test results showed a significant similarity between the SCB CHM and NCC methods; hence, SCB CHM can be used as a reliable test alternative for QA/QC measurements.

Study results indicated that the SCB CHM test will produce results similar to those measured using SCB NCC. The SCB CHM can be used as a QA/QC test of fracture properties of asphalt mixtures and the J_c value can be measured accurately.

CHAPTER 3

HOT-APPLIED MODIFIED BINDER CHIP-SEAL FIELD PERFORMANCE IN CALIFORNIA

The objective of this chapter was to assess current conditions of the 14 California Department of Transportation (Caltrans) modified binder (MB) seal-coat projects, which contained some amount of crumb rubber modified (CRM), and determine their field performance. Field reviews of these projects were conducted between September and October 2015. Most projects were rated either good or fair, but some projects were rated poor. The primary distress types were transverse cracking, bleeding, and longitudinal cracking. Also, streaking and roping due to improper application rate/construction were observed. Based on the study, transverse cracking and bleeding were the dominant distresses in high-mountain and high-desert regions.

Chip seal is among the most commonly used pavement preservation treatment in California. It enhances skid resistance, arrests raveling, and seals minor cracks (Caltrans, 2008b). Kodippily (2013) conducted a survey in several countries that used chip seal and found that aggregate loss and bleeding were the most common distresses associated with the performance of chip seal. Several researchers indicated that the use of PM binder would improve chip retention (Khattak, Baladi, & Drzal, 2007; Takamura, 2003; Yildirim, 2007).

Pavement with PM asphalt tends to have better fatigue resistance, lower fatigue cracking, and less stripping. It is due to these advantages that PM asphalt is used in areas of critical loading such as intersections, weigh stations, and race tracks (SHRP, 2017). The U.S. Army Corps of Engineers indicated it is advantageous to use an asphalt modifier that would increase the life of

the pavement and reduce costs (King, King, Pavlovich, Epps, & Kandhal, 1999). PM was found to be a good choice to enhance fatigue resistance.

Several researchers used CRM binder for the application of chip seal. Properties of CRM binder are influenced by asphalt composition, type, and size of the CRM and the reaction time and temperature (Khattak et al., 2007; Partl & Newman, 2003; Yilidrim, 2007). In California, approximately 40 million scrap tires per year are generated (Industrial Resource Council, as cited in Becker, Méndez, & Rodriguez, 2001). According to the Environmental Protection Agency, the three largest scrap-tire markets are tire-derived fuel, civil engineering applications, and ground rubber applications/rubberized asphalt (Industrial Resources Council). Asphalt rubber is the largest single market for ground rubber (Caltrans, 2008a). Ground tire rubber can be blended with asphalt to beneficially modify the properties of the asphalt in highway construction. Use of scrap tires into asphalt will reduce the waste problem (Caltrans, 2013). At the same time, it is expected to produce long-lasting asphalt mixtures that perform similar or better than mixtures containing no rubber (Caltrans, 2015a).

Caltrans has used MB seal coats containing either polymers or CRM since 2008 and has constructed a number of projects in several districts. The normal practice in California is to use single-chip seal, which consists of an application of binder followed by an application of aggregate (Lane & Cheng, 2015a). However, an MB chip-seal coat that consists of an application of a modified-binder (MB) and precoated screenings (medium and hot applied) followed by a flush coat (asphalt emulsion and sand cover) has been used. In 2015, Caltrans tasked the California Pavement Preservation (CP2) Center to assess the current conditions and performance of 14 Caltrans MB seal-coat projects that contained some amount of CRM. The majority of these

projects were constructed between 2009 and 2012 (Carstens & Rahim, 2015a, 2015b; Lane & Cheng, 2015b; Saadeh & Eljairi, 2015).

Objective

The objective of this study was to assess the current conditions of the listed Caltrans MB seal-coat projects that contained some amount of CRM, and determine their field performance.

Project Information

Location, Traffic, Climate, and Preexisting Pavement Structure

Table 11 shows the location, and the 2014 traffic data, which includes annual average daily traffic (AADT) and percentage of truck information. The table also contains climate region.

Table 11

List of Modified Binder Seal-Coat Projects Evaluated in 2015

Project ID#	Location (county, highway)	Length, km	AADT	Truck, %	Climate region	Construction month/year
02-0E5704	Siskiyou (SIS), 96	8.50	680–830	9.6–36.1	High Mountain	Oct. /2009
02-0E5704	Tehama (THE), 36	7.45	700–1,650	11.2–19.7	High Mountain	
02-3E6804	Trinity (TRI), 03	9.30	1,400–2,200	45.7	Low Mountain	Aug. /2011
02-3E0104	Lassen (LAS), 36	1.30	4,600–12,000	3.8–7.6	High Desert	
02-3E9104	Siskiyou (SIS), 89	5.35	2,500–3,050	13.4–16.5	High Mountain	Sept. /2012
02-3E9104	Trinity (TRI), 03	3.73	1,050–3,750	4.6–8.0	Low Mountain	
03-3M8804	El Dorado (ED), 193	5.60	3,000–3,500	4.4–5.3	Low Mountain	Sept. /2011
03-3M8904	Yolo (YOL), 113	6.65	3,600–10,400	7.0–15.9	Inland Valley	Aug. /2011
05-0Q9504	San Luis Obispo (SLO), 227	3.85	3,010	5.3	Central Coast	Aug. /2009
05-0T4004	San Luis Obispo (SLO), 01	14.30	3,000	3.7	Central Coast	Nov. /2012
05-1A4204	Monterey (MON), 198	11.68	870	11.6	Inland Valley	Sept. /2012
06-0L1204	Kern (KER), 184	1.37	3,560	17.7	Inland Valley	Jun. 2010
06-0L1204	Kern (KER), 223	3.67	3,188	NA[1]	Inland Valley	
06-0L1404	Kern (KER), 155	16.40	331	NA	South Mountain	Nov. /2011
09-339404	Inyo (INY), 168	Various	400–7650	1.0–11.3	High Desert	Feb. /2010
09-339404	Mono (MNO)), 226		140–200	2.86–6.0	High Desert	
09-342804	Mono (MNO), 395	13.86	3,100–3,600	7.4–10.8	High Desert	Jul. /2012
09-347104	Mono (MNO), 395	8.76			High Desert	Jul. /2011

Note. AADT = annual average daily traffic, [a]Truck data not available

Materials

Based on the special provisions of the projects, the supplier is required to certify a minimum of 10% CRM from waste tires in the binder and the MB is required to meet a typical PG 76-22 specification. Table 12 lists the graduation requirements for aggregate screenings used and Table 13 lists the application rates of seal-coat materials. Note that all the information included in these tables was obtained from the project special provisions. Actual application rates

were back-calculated from project construction-cost records and included in Table 14. Actual material testing data were not available for inclusion.

Table 12

Screening Gradation Requirement Based on Project Special Provisions

Project ID #	02-0E5704 02-3E9104 05-0Q9504	09-342804	02-2E6804 02-3E0104 03-3M8904 05-0T4004 05-1A4204 06-0L1404 06-0L1204	03-3M8804 09-339404	09-347104
Sieve Sizes	3/8” Max size; % passing	3/8” Max size; % passing	3/8” Max size; % passing	1/2” Max size; % passing	5/16” Max size; % passing
3/4”	—		100	100	—
1/2”	100	100	95–100	85–90	100
3/8”	85–100	90–100	70–85	0–30	95–100
No. 4	0–15	5–30	0–15	0–5	0–50
No. 8	0–5	0–10	0–5	—	0–15
No. 16	—	0–5	—	—	0–5
No. 30	—		—	—	0–3
No. 200	0–2	0–2	0–1	0–1	0–1

Table 13

Materials Application Rates Based on Project Special Provisions

Project ID #	MB application rate; l/m^2	Screening application rate; kg/m^2	Sand-cover application rate; kg/m^2	Fog-seal-coat application rate; l/m^2
02-0E5704	≤ 2.31	≤ 21.01	≤ 2.44	≤ 0.27
02-2E6804	1.36–1.90	9.77–14.10	1.09–2.17	0.09–0.14
02-3E0104	1.36–1.90	9.77–14.10	1.09–2.17	0.09–0.14
02-3E9104	1.36–1.90	9.77–14.10	1.09–2.17	0.09–0.14
03-3M8904	1.36–1.90	9.77–14.10	1.09–2.17	0.09–0.14
03-3M8804	1.13–1.81	10.86–16.29	1.09–2.17	0.09–0.18
05-0T4004	1.36–1.90	9.77–14.10	1.09–2.17	0.02–0.03
05-0Q9504	≤ 2.31	≤ 21.01	≤ 0.27	≤ 0.27
05-1A4204	1.36–1.90	9.77–14.10	1.09–2.17	0.09–0.14
06-0L1404	1.36–1.90	9.77–14.10	1.09–2.17	0.09–0.14
06-0L1204	1.36–1.90	9.77–14.10	1.09–2.17	0.09–0.14
09-339404	1.58–2.26	10.86–18.46	1.09–2.17	0.14–0.27
09-342804	2.04	8.69–13.03	1.09–2.17	0.09–0.14
09-347104	1.13–1.45	8.69–13.03	1.09–2.17	0.09–0.14

Note. MB = modified binder.

Table 14

Actual Material Application Rates Calculated From Construction Records

Project ID #	MB application rate; l/m^2	Screening application rate; kg/m^2	Sand-cover application rate; kg/m^2	Fog-seal-coat application Rate; l/m^2
02-0E5704	1.68	13.69	0.98	0.14
02-2E6804	1.61	13.52	2.02	0.27
02-3E0104	1.43	12.98	1.83	0.23
02-3E9104	1.68	10.32	0.98	0.14
03-3M8904	1.00	9.12	1.15	0.09
03-3M8804	1.86	13.97	1.48	0.24
05-0T4004	1.27	10.48	0.50	0.11
05-0Q9504	1.49	13.09	1.98	0.26
05-1A4204	1.58	13.09	1.79	0.18
06-0L1404	1.22	10.70	1.31	0.15
06-0L1204	1.04	7.91	0.69	0.11
09-339404	2.15	17.43	2.83	0.22
09-342804	2.28	16.83	2.83	0.34
09-347104	2.48	16.62	2.53	0.33

Note. MB = modified binder.

Review Approach

The approach to the field review included a manual rating of the surface condition and distresses in these seal coats, through a random sampling of roadway segments. Each sampling location was called a performance evaluation section (PES) and was about 3.6-m (12-feet) wide and 30.50-m (100-feet) long. For each project, multiple PESs were used to represent the overall condition of the project. Field observations were recorded on a form developed for the review.

Distress Types

The review focused on the following surface conditions or indicators that might potentially relate to or reflect seal-coat performance such as cracking, raveling/rock loss,

flushing/bleeding and streaking/roping. uniformity of the surface texture, chip embedment, and other types of distresses (if any) were also noted during the review.

Rating System

A rating system using a scale of very good to excellent, good, fair, and poor was developed. The following are the definitions of the ratings:

Very good to excellent: The seal coats have a tight and uniform surface texture, good chip embedment, and are free of cracking, raveling, flushing, or roping. There may be one type of low severity and a small quantity of distress in the form of low severity hairline cracking or minimal roping. No indication emerged that rock loss has occurred.

Good: The seal coats have a slightly rough surface texture and good chip embedment. The seal coats have no more than two types of low severity and small quantity of distress, for example, surface texture and hairline cracking or marginal embedment with indications of roping. No indication emerged of rock loss, flushing, or bleeding.

Fair: The seal coats have a rough surface texture and fair chip embedment. They have no more than two types of medium severity and a moderate quantity of distress. An indication emerged that rock loss had occurred but is not continuing to occur; or cracking where crack sealing may be required; or the seal coats have three types of low severity and a small quantity of distress, such as hairline cracking, rock loss, and minor flushing.

Poor: The seal coats have a very rough surface texture and poor chip embedment. More than two types of medium severity emerged and a moderate quantity of distresses. One or more types of high severity and large quantities of cracks emerged where cracked sealing is required, along with obvious signs of continuing rock loss, signs of flushing due to rock loss, and severe raveling.

Review Method

the review was performed through visual inspection from the shoulder on preidentified PESs locations. the preidentified PESs, were randomly selected and located using Caltrans iVision software or Google Map/Earth. For work safety, the PES locations had sufficient shoulder space for vehicle parking.

Depending on the length of the project being reviewed four to 16 PESs for both travel directions, were identified, to represent the surface condition of the entire project. a drive-through and windshield survey of the project were also conducted to document any major surface distresses and overall condition of the roadway. significant localized problem areas were noted. The survey team also took photographs to show the major distresses of pavement and document other significant information.

Survey-Results Summary

The overall performance ratings for the total of 18 locations in five Caltrans districts appear in Table 15. The overall rating of each project is the median rating of all PES ratings for the project. The detailed survey results, including photographs and field-survey forms, are in the individual district report, shown in the reference section of this paper.

Table 15

PES Ratings for Modified-Binder Seal-Coat Projects

District ID	Location	AADT	Years of service	Overall rating
02-0E5704	SIS 96 (North of Yreka)	680–830	6	Good
02-0E5704	TEH 36 (East of Mineral)	700–1,650	6	Poor
02-2E6804	TRI 3 (West of Douglas City)	1,400–2,200	4	Good
02-3E0104	LAS 36 (Near Susanville)	4,600–12,000	4	Poor
02-3E9104	SIS 89 (Near McCloud)	2,500–3,050	3	Good
02-3E9104	TRI 3 (Near Weaverville)	1,050–3,750	3	Good
03-3M8804	ED 193 (Georgetown to Kelsey)	3,000–3,500	4	Fair
03-3M8904	YOL 113 (Near Woodland)	3,600–10,400	4	Poor
05-0Q9504	SLO 227 (Near Arroyo Grande)	3,010	6	Good
05-0T4004a	SLO 1 (Near Cambria)	3,000	3	Very Good
05-1A4204	MON 198 (Near San Lucas)	870	3	Good
06-0L1204	KER 184 (At Wheeler Bridge Rd)	3560	5	Poor
06-0L1204	KER 223 (Between SR 99 and I-5)	3,188	5	Poor
06-0L1404	KER 155 (Near Sequoia National Park)	331	4	Fair
09-339404b	INY 168 (Near Bishop)	400–7650	5	Fair
09-339404b	MNO 266 (Near Bishop)	140–200	5	Fair
09-342804	MNO 395 (Near Walker)	3100–3600	4	Good
09-347104	MNO 395 (Near Walker)	3100–3600	4	Poor

Note. AADT = annual average daily traffic, [a]A sand seal was placed on top of the modified-binder seal coat in October/November 2013. [b] 09-339404 was a field-blended tire rubber.

Performance By District, Climatic Region, Pavement Age, and Traffic Level

MB Seal-Coat Performance by District

Results from the visual survey revealed MB seal-coat projects performed differently among Caltrans districts. The Following summarizes the performance of MB projects in each Caltrans district.

District 02 MB Seal Coat Projects

The performance of the MB seal-coat projects in District 02 was rated from Good to Poor in 2015. One 6-year-old project (SIS 96) was rated Good; one 6-year-old project (TEH 36) was rated Poor; one 4-year-old project (TRI 3) was rated Good; one 4-year-old project (LAS 36) was rated Poor; and two 3-year-old projects (TRI 3 and SIS 89) were rated Good.

The Major distresses found in District 02 MB seal-coat projects, based on the number of PES observations, in descending order, were bleeding, transverse cracking, streaking/roping, delamination, longitudinal cracking, and fatigue cracking, shown in Figure 14. The most dominant distresses were bleeding and transverse cracking. Some apparent bleeding in the wheel paths may be due to rock loss from chain wear, where the chips were removed by chains or snow plows. The transverse cracking was normally due to reflective cracking or thermal cracking from high temperature differentials in the region. As shown in Tables 13 and 14 some sections in Districts 02 and 03 had fog-seal-coat applications that were higher than the standard application rates. This could have led to the bleeding distresses observed in these sections.

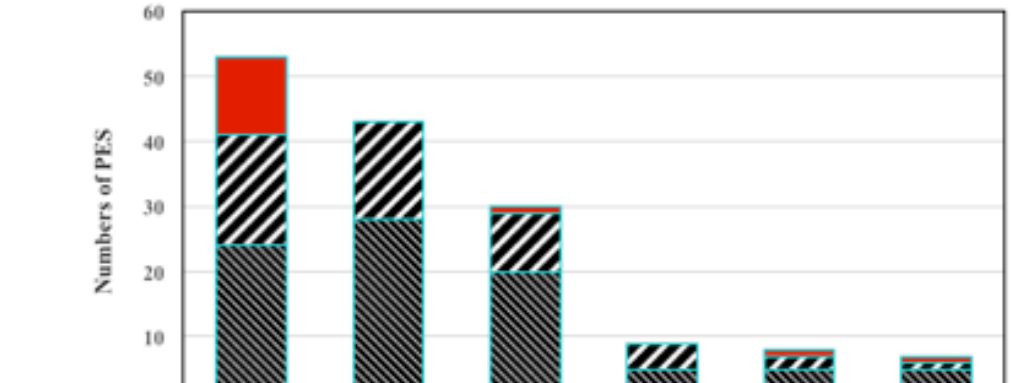

	Bleeding	Transverse Cracking	Streaking/ Roping	Delamination	Longitudinal Cracking	Fatigue Cracking
High Severity	12		1		1	1
Medium Severity	17	15	9	4	2	1
Low Severity	24	28	20	5	5	5

Figure 14. Distress ranking for surveyed modified-binder seal-coat projects in District 02.

District 03 MB Seal-Coat Projects

The performance of the two 4-year-old MB seal-coat projects (YOL 113 and ED 193) in District 03 was rated as Fair and Poor, respectively, in 2015. The major distresses found in District 03 MB seal-coat projects, based on the number of PES observations, in descending order, were transverse cracking, bleeding, longitudinal cracking, block cracking, fatigue cracking, and reflective cracking, shown in Figure 15. The most dominant distresses were transverse cracking and bleeding. Some apparent bleeding in the wheel paths may be due to rock loss. The transverse cracking could be due to reflective cracking or thermal cracking from high temperature differentials in the region, and traffic actions. As seen in Tables 13 and 14, one section (03-3M8904) had application rates that were lower than the standard rates for all materials used in the MB chip-seal construction. This section experienced high levels of all types of cracking (transverse, block, and alligator) which are probably reflection cracking. However, in section 03-3M8804, which has a high application rate of MB and fog seal coat, bleeding was the dominant distress.

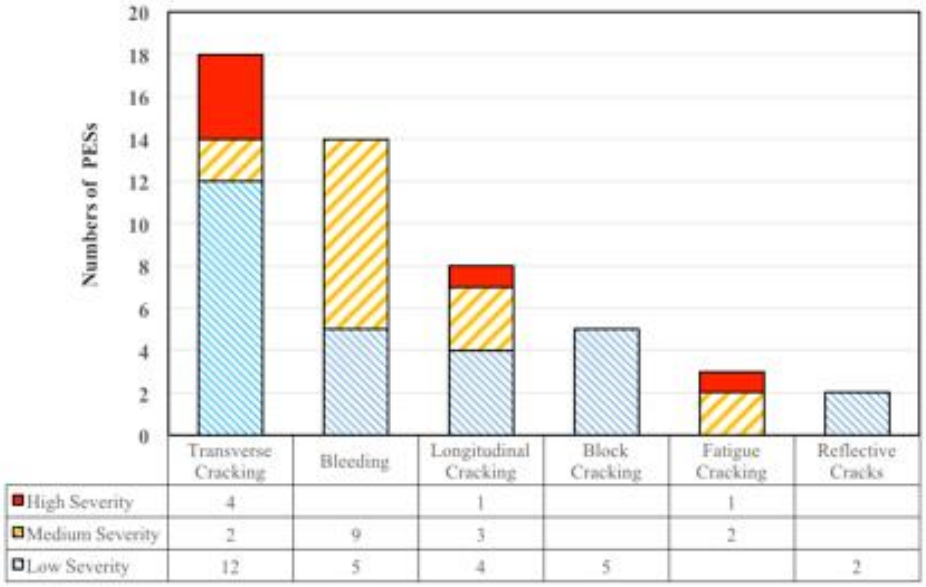

Figure 15. Distress ranking for surveyed modified-binder seal-coat projects in District 03.

District 05 MB Seal-Coat Projects

The performance of the MB seal-coat projects in District 05 was rated Very Good to Good in 2015: one 6-year-old project (SLO 227) was rated Good; one 3-year-old project (SLO 01) was rated Very Good and one 3-year-old project (MON 198) was rated Good. The SLO 01 project received a sand seal in October/November 2013. The major distresses found in District 5 MB seal-coat projects, based on the number of PES observations, in descending order, were transverse cracking, streaking/roping, rutting, longitudinal cracking, bleeding, and segregation, shown in Figure 16. The most dominant distresses were transverse cracking and streaking. The transverse cracking was likely due to reflective cracking. The streaking/roping was likely related to possible uneven application of the binder during the construction.

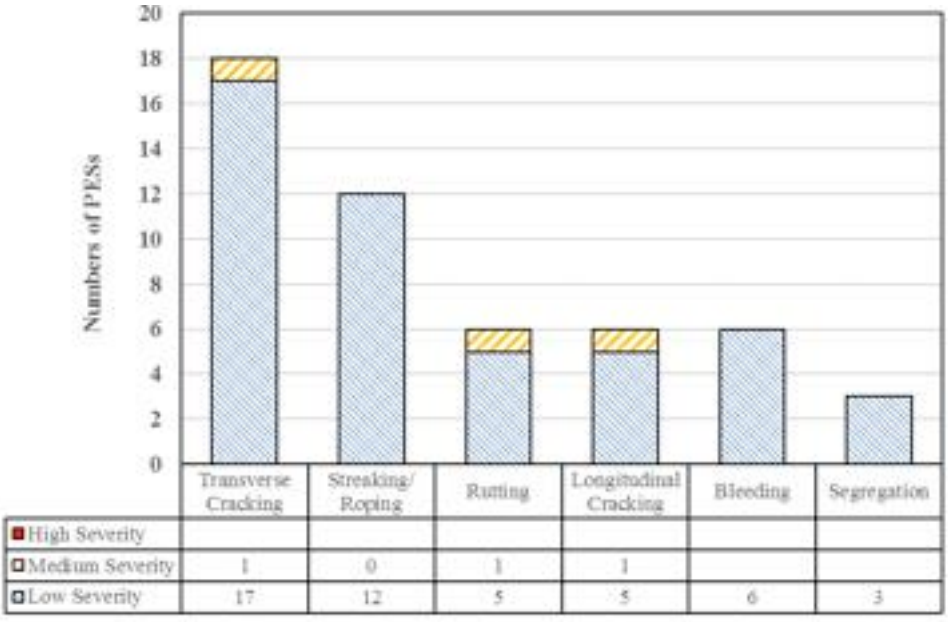

Figure 16. Distress ranking for surveyed modified-binder seal-coat projects in District 05.

District 06 MB Seal-Coat Projects

The performance of the MB seal-coat projects in District 06 was rated from Fair to Poor in 2015: one 4-year-old project (KER 155) was rated Fair; and two 5-year-old projects (KER 184

and KER 223) were rated Poor. The major distresses found in District 06 MB seal-coat projects, based on the number of PES observations, in descending order, were transverse cracking, longitudinal cracking, streaking/roping, bleeding, fatigue cracking, and block cracks, shown in Figure 17. The most dominant distresses were transverse and longitudinal cracking. The transverse and longitudinal cracking was likely due to reflective cracking and environment-caused distresses, such as thermal cracking. The application rate of MB and screening was at the low limit of the standard rate of application, which could have led to the accelerated deterioration in these two sections.

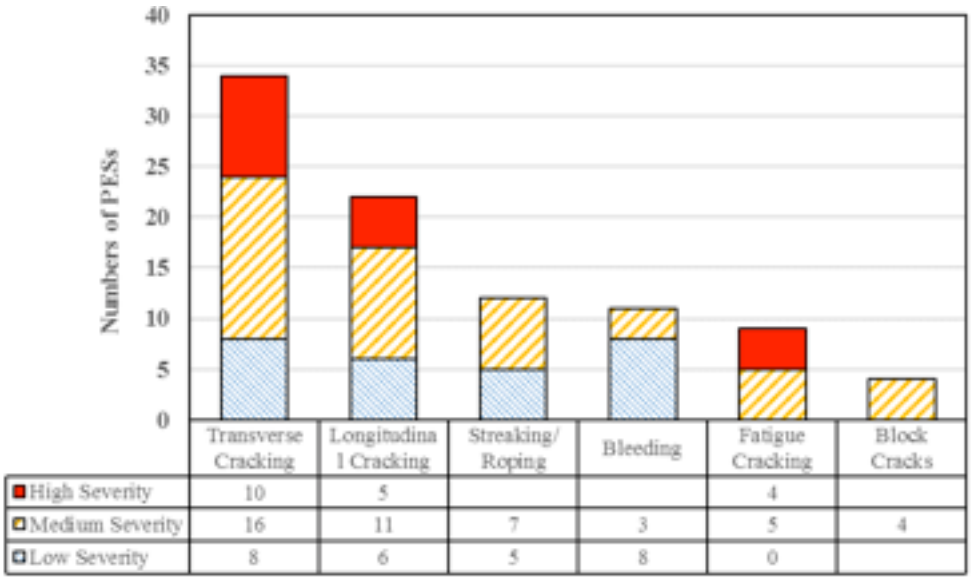

Figure 17. Distress ranking for surveyed modified-binder seal-coat projects in District 06.

District 9 MB Seal-Coat Projects

The performance of the MB seal coat projects in District 09 was rated from Good to Fair in 2015: two 5-year-old projects (INY 168 and MNO 266) were rated Fair; one 4-year-old project (MNO 395) was rated Poor; and one 4-year-old project (MNO 395) was rated Good. The major distresses found in District 09 MB seal-coat projects, based on the number of PES

observations, in descending order, were transverse cracking, bleeding, streaking/roping, longitudinal cracking, raveling and polished aggregate, shown in Figure 18. The most dominant distresses were transverse cracking and bleeding. Transverse cracking was likely due to high temperature differentials or thermal cracking. The apparent bleeding could be due to the high application rates used. Also, the application rate for screening and sand cover were at or higher than the upper limit of standard rates, which could have led to rock loss and the rough surface observed during the visual survey.

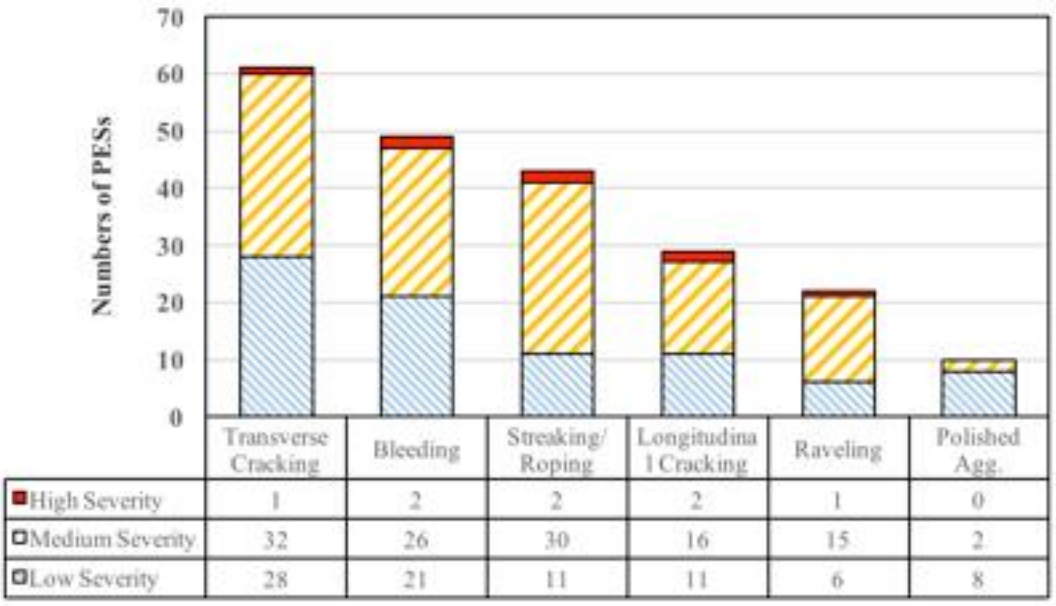

	Transverse Cracking	Bleeding	Streaking/ Roping	Longitudinal Cracking	Raveling	Polished Agg.
High Severity	1	2	2	2	1	0
Medium Severity	32	26	30	16	15	2
Low Severity	28	21	11	11	6	8

Figure 18. Distress ranking for surveyed modified-binder seal-coat projects in District 9.

MB Seal-Coat Performance in Different Climate Regions

MB seal-coat projects were located in the different climate regions of high mountain, low mountain, south mountain, high desert, desert, inland valley, and central coast. Overall, the most dominant distress was transverse cracking, except in some high mountain regions, where apparent bleeding was the dominant distress from rock loss due to snow chains or snow plows. The transverse cracking was likely due to high temperature differentials or thermal cracking in

high-mountain, high-desert, and some inland-valley climate regions. MB seal coats appeared to perform well in the central coast region due to its temperate weather.

MB Seal-Coat Performance and Traffic Level

Traffic had a major impact on the performance of these surveyed MB seal-coat projects. The seal coats performed poorly under high-traffic volumes such as YOL 113 near Woodland and LAS 36 near Susanville, where AADTs were more than 10,000 vehicles per day. The heavy truck traffic could also contribute to the deterioration of seal coats, such as KER 184 at Wheeler Bridge Rd. and KER 223 between SR 99 and I-5.

MB Seal-Coat Performance and Pavement Age

Pavement age had some impact but was not the only factor impacting the performance of the reviewed MB seal-coat projects. All 3-year-old projects performed Good whereas 4- to 6-year-old projects performed in various ways. In the same high-mountain regions in District 02, SIS 96 at north of Yreka performed good after 6 years of service whereas the project on TEH 36 east of Mineral performed poorly after 6 years of service. The 6-year-old project SLO 227 near Arroyo Grande performed almost as well as the 3-year-old project on SLO 1 near Cambria, which also received a sand-seal application in October/November 2013. These two projects had almost the same AADT. However, projects built in District 06 with 5 years in service performed poorly despite having an AADT close to that for District 05 projects. The main reason behind such performance could relate to the much higher truck percentage on District 06 projects compared to those built in District 05.

Conclusions

Field performance of 14 MB seal-coat projects containing polymers or CRM in several Caltrans districts in this study. The following preliminary conclusions from the collected and analyzed data:

- The field review included a performance assessment of 14 projects at 18 locations in five Caltrans districts.
- For each project, multiple randomly selected PESs were used to represent the overall surface condition of the project. the review was performed on PESs through visual inspection and rated each PES, based on the surface condition. The median rating represented the overall rating of the project.
- The majority of these projects have been in service for 3 to 6 years and their overall performance was mixed. This mixed performance was likely due to the varying geometric conditions, varying environmental condition of the highway, and varying traffic and preexisting pavement conditions.
- Of the 18 locations reviewed, eight were rated Good; four were rated Fair; and six were rated Poor.
- The primary distress types were transverse cracking, bleeding, streaking/roping, and longitudinal cracking. The dominant distress was transverse cracking, followed by bleeding.
- Transverse cracking and bleeding were the dominant distresses in high-mountain and high-desert regions.
- High traffic volume, especially heavy trucks, could have contributed to the wearing of seal coats.

- Application rates of the different materials used in MB chip seal for several sections were either lower or higher than the standard rates of application. This construction deficiency could have led to the various distresses observed.

I recommend the following as a result of this evaluation:

- MB seal coats appear to slow down the deterioration of existing pavement surfaces. Further applications of seal coats, if appropriate, should be considered to preserve pavement surfaces.
- Crack seal, if applicable, should be applied prior to a seal coat.
- To determine the effectiveness of the seal coats, the condition of the existing pavement should be assessed and recorded for future comparison.
- The construction records, actual material testing data, and application rates of seal coats should be retained for performance evaluation.

REFERENCES

Arabani, M., & Ferdowsi, B. (2009). Evaluating the semi-circular bending test for HMA mixtures. *International Journal of Engineering A: Basics, 22*(1). 47–58.

ARAMIS [Computer software]. King of Prussia, PA: Trillion Quality Systems.

Becker, Y., Méndez, M. P., & Rodríguez, Y. (2001). Polymer modified asphalt. *Vision Technologica, 9*(1), 39–50.

Breiman, L., & Cutler, A. (1984) *Random forests.* Retrieved June 18, 2019, from https://www.stat .berkeley.edu/~breiman/RandomForests/cc_home.htm

Brown, E. R., Kandhal, P. S., Roberts, F. L., Kim, Y. R., Lee, D. Y., & Kennedy, T. W. (2009). *Hot mix asphalt materials, mixture design and construction* (3rd ed.). Lanham, MD, US: NAPA Research and Education Foundation.

California Department of Transportation. (2008a). *Asphalt rubber usage guide.* Sacramento, CA, US: Author. Retrieved July 22, 2016, from http://www.dot.ca.gov/hq/esc/Translab/ormt /pdf/Caltrans_Asphalt_Rubber_Usage_Guide.pdf

California Department of Transportation. (2008b). *Maintenance technical advisory guide. Volume I – Flexible pavement preservation* (2nd ed.). Sacrament, CA, US: Author. Retrieved July 22, 2016, from http://www.dot.ca.gov/hq/maint/MTA _GuideVolume1Flexible.html

California Department of Transportation. (2015a). *Chapter 5: Chip seals.* Retrieved October 15, 2015, from http://www.dot.ca.gov/hq/maint/mtag/ch5_chip_seals.pdf

California Department of Transportation. (2015b). *Standard specifications.* Sacramento, CA, US: State of California, Business, Transportation and Housing Agency.

California Department of Transportation, Division of Maintenance. (2013). *State of the pavement report based on the 2013 Pavement condition survey.* Retrieved from http://www.dot.ca.gov/hq/maint/Pavement/Pavement_Program/PDF/2013_SOP_FINAL-Dec_2013-1-24-13.pdf

Carstens, K., & Rahim, A. (2015a). Performance evaluation of modified binder seal coat projects in District 05 (Technical Report 2015–107). Chico, CA, US: California Pavement Preservation Center.

Carstens, K., & Rahim, A. (2015b) Performance evaluation of modified binder seal coat projects in District 06 (Technical Report 2015–108). Chico, CA, US: California Pavement Preservation Center.

Chong, K. P., & Kuruppu M. D. (1984). New specimen for fracture toughness determination for rock and other materials. *International Journal of Fracture, 26,* R59–R62. https://doi.org/10.1007/BF01157555

Elkins, G. E., Thompson, T., Ostrom, B., Simpson, A., & Visintine, B. (2017). *Long-term pavement performance: Information management system user guide* (Publication No. FHWA-RD-03-088). McLean, VA: Federal Highway Administration.

Géron, A. (2017). *Hands-on machine learning with Scikit-Learn and TensorFlow: Concepts, tools, and techniques to build intelligent systems.* Sebastopol, CA: O'Reilly Media.

Haider, S. W., & Chatti, K. (2009). Effect of design and site factors on fatigue cracking of new flexible pavements in the LTPP SPS-1 experiment. *International Journal of Pavement Engineering, 10*(2), 133–147. https://doi.org/10.1080/10298430802169390

Hakimelahi, H., Saadeh, S., & Harvey, J. (2013). Comparison of fracture properties of four point beam and semi circular bending of asphalt concrete. *Journal of Road Materials and Pavement Design, 14*(2), 252–265. https://doi.org/10.1080/14680629.2013.812835

Harvey, J. T., Deacon, J. A., Tsai, B. W., & Monismith, C. l. (1995). *Fatigue performance of asphalt concrete mixes and its relationship to asphalt concrete pavement performance in California.* Berkeley, CA, US: University of California, Institute of Transportation Studies Asphalt Research Program.

Hofman, R., Oostcrbaan, B., Erkens, S., & Kooji, J. (2003). *Semi-circular bending test to assess the resistance against crack growth.* Delft, The Netherlands: Road and Hydraulic Engineering Institute, Directorate Public Works and Water Management.

Industrial Resources Council. *Rubber manufacturing.* Retrieved July 22, 2016, from http://www.industrialresourcescouncil.org/IndustrySector /RubberManufacturing/tabid/373/Default.aspx

Ker, H.-W., Lee, Y.-H., & Wu, P.-H. (2008). Development of fatigue cracking prediction models using long-term pavement performance database. *Journal of Transportation Engineering, 134*(11), 477–482. https://doi.org/10.1061/%28ASCE%29TE.1943-5436.131

Khattak, M. J., Baladi, G. Y., & Drzal, L. T. (2007). Low temperature binder-aggregate adhesion and mechanistic characteristics of polymer modified asphalt mixtures. *Journal of Materials in Civil Engineering, 19*(5), 411–422. https://doi.org/10.1061/(ASCE)0899 -1561(2007)19:5(411)

Khattak, M. J., & Peddapati, N. (2013). Flexible pavement performance in relation to in situ mechanistic and volumetric properties using LTPP data. *ISRN Civil Engineering,* Art. 972020. https://doi.org/10.1155/2013/972020

Kim, M., Mohammad, L. N., & Elseifi, M. A. (2012). Characterization of fracture properties of asphalt mixtures as measured by semicircular bend test and indirect tension test. *Transportation Research Record, 2296*(1), 115–124. https://doi.org/10.3141/2296-12

King, G., King, H., Pavlovich, R. D., Epps, A. L., & Kandhal, P. S. (1999). Additives in asphalt. *Journal of the Association of Asphalt Paving Technology, 68,* 32–69.

Kodippily, S. (2013). *Modelling the flushing mechanism of thin flexible surface pavements* (Unpublished doctoral dissertation). The University of Auckland, Auckland, New Zealand.

Lane, L., & Cheng, D. (2015a). *Performance evaluation of modified binder seal coat projects in District 02* (Technical Report 2015–105). Chico, CA, US: California Pavement Preservation Center.

Lane, L., & Cheng, D. (2015b). *Performance evaluation of modified binder seal coat projects in District 03* (Technical Report 2015–106). , Chico, CA, US: California Pavement Preservation Center.

Mahmoud, E., Saadeh, S., & Hakimelahi, H. (2013). Extended finite element modeling of asphalt mixtures fracture properties using the semi-circular bending test. *Journal of Road Materials and Pavement Design, 15*(1), 153–166. https://doi.org/10.1080/14680629.2013.863737

MATLAB (1984) [Computer software]. Natick, MA, US: MathWorks.

Miller, J. S., Bellinger, W. Y. (2003). *Distress identification manual for the long-term pavement performance program* (4th rev. ed., Publication No. FHWA-RD-03-031). McLean, VA, US: Federal Highway Administration.

Mohammad, L. N., Negulescu, I, Wu, Z., Daranga, C., Daly, W. H., & Abadie, C. (2003). Investigation of the use of recycled polymer modified asphalt binder in asphalt concrete pavements. In *Proceedings of the Technical Sessions, Asphalt Paving Technology.* Lino Lakes, MN, US: Association of Asphalt Paving Technologists.

Mohammad, L. N., Wu, Z., & Aglan, M. (2004). Characterization of fracture and fatigue resistance on recycled polymer-modified asphalt pavements. In C. Petit, I. L. Al-Qadi, & A. Millien (Eds.), *Fifth international RILEM conference on reflective cracking in pavements* (pp. 375–382). Limoges, France: RILEM.

Mohammad, L. N., Kabir,M.D., And Saadeh,S. (2008). Evaluation of fracture properties of HMA. *Fifth international RILEM conference on reflective cracking in pavements* (pp. 375–382). Limoges, France: RILEM.

Molenaar, A., Scarpas, A., Liu, X., & Erkens, S. M. J. G. (2002). Semi-circular bending test: Simple but useful? *Journal of the Association of Asphalt Paving Technologists, 71,* 794–815.

Mull, M. A., Stuart, K., & Yehia, A. (2002). Fracture resistance characterization of chemically modified crumb rubber asphalt pavement. *Journal of Materials Science*, *37*(3), 557–566. https://doi.org/10.1023/A:1013721708572

National Cooperative Highway Research Program. (2016). *Experimental design for field validation of laboratory tests to assess cracking resistance of asphalt mixtures* (NCHRP 09-57). Washington, DC: National Cooperative Highway Research Program.

Othman, A. (2011). Evaluation of hydrated lime effect on the performance of rubber-modified HMA mixtures. *Journal of Elastomers & Plastics*, *43*(3), 221–237. https://doi.org/10 .1177/0095244311398628

Paris, P. C., & Erdogan, F. (1963). A critical analysis of crack propagation laws. *Journal of Basic Engineering, 85*(4), 528–534. https://doi.org/10.1115/1.3656900

Park, H. J., & Kim, Y. R. (2015). Primary causes of cracking of asphalt pavement in North Carolina: Field study. *International Journal of Pavement Engineering, 16,* 684–698. https://doi.org/10.1080/10298436.2014.943220

Partl, M. N., & Newman, J. K. (2003). Flexural beam fatigue properties of airfield asphalt mixtures containing styrene–butadiene based polymer modifiers. In M. di Prisco, R. Felicetti, & G. A. Plizzari (Eds.), *Proceedings of the 6th International RILEM Symposium* (pp. 357–363). Zurich, Switzerland: RILEM.

The R Foundation. (2019). *The R project for statistical computing.* Retrieved January 1, 2019, from https://www.r-project.org/

Roberts, F., Kandhal, P., Brown, E., Lee, D., & Kennedy, T. (2009). *Hot mix asphalt materials, mixture design and construction.* Lanham, MD, US: National Center for Asphalt Technology.

Saadeh, S., & Eljairi, O. (2015). *Performance evaluation of modified binder seal coat projects in District 9* (Report Number: CP2C-2015–109). Chico, CA, US: California Pavement Preservation Center.

Saadeh, S., Eljairi, O., Kramer, B., & Hajj, E. (2012). Development of quality control test procedure for characterizing fracture properties of asphalt mixtures. In *Four-point bending—Proceedings of the 3rd Conference* (pp. 223–238). Davis, CA, US, University of California. https://doi.org/10.1201/b12767-24

Saha, G., & Biligiri, K. P. (2017). Cracking performance analysis of asphalt mixtures using response surface methodology: Experimental investigations and statistical optimization. *Materials and Structures, 50,* 1–12. https://doi.org/10.1617/s11527-016-0906-5

Simpson, A. L., Schmalzer, P. N., & Rada, G. R. (2007). *Long term pavement performance project laboratory materials testing and handling guide* (Publication No. FHWA-RD-07-1541). McLean, VA, US: Federal Highway Administration.

Strategic Highway Research Program. (2017). Superpave mix design—Level 1 (low traffic). Washington, DC: Author.

Svetnik, V., Liaw, A., Tong, C., Culberson, J. C., Sheridan, R. P., & Feuston, B. P. (2003). Random forest: A classification and regression tool for compound classification and QSAR modelling. *Journal of Chemical Information and Modeling, 43,* 1947–1958. https://doi.org/10.1021/ci034160g

Takamura, K. (2003, March). Improved fatigue resistance of asphalt emulsion residue modified with SBR latex. Paper presented at the annual meeting of Asphalt Emulsion Manufacturers Association, Nashville, TN.

Wagnoner, M. P., Buttlar,W. G., & Paulino, G. H. (2005). Disk-shaped compact tension test for asphalt concrete. *Experimental Mechanics, 45,* 270–277. https://doi.org/10.1007 /BF02427951

Wu, Z., Mohammad, L. N., Wang, L. B., & Mull, M. A. (2005). Fracture resistance characterization of Superpave mixtures using the semi-circular bending test. *Journal of ASTM International, 2*(3), 1–15. https://doi.org/10.1520/JAI12264

Yildirim, Y. (2007). Polymer modified asphalt binders. *Construction and Building Materials, 21*(1), 66–72. https://doi.org/10.1016/j.conbuildmat.2005.07.007

Zelelew, H., Senn, K., & Papagiannakis, T. (2012). Forensic evaluation of the LTPP specific pavement study projects in Arizona. *Journal of Performance of Constructed Facilities, 26*, 668–678. https://doi.org/10.1061/%28ASCE%29CF.1943-5509.0000288

Zeng, G., Yang, X., Chen, L., & Bai, F. (2016). Damage evolution and crack propagation in semicircular bending asphalt mixture specimens. *Acta Mechanica Solida Sinica, 29*, 596–609. https://doi.org/10.1016/S0894-9166(16)30330-5

Zhou, F., Hu, S., & Scullion, T. (2007). *Development and verification of the overlay tester based fatigue cracking prediction approach* (Report FHWA/TX-07/9-1502-01-8). College Stations, TX, US: Texas Transportation Institute.